

QUASARS AND ROTATING BLACK HOLES *

Max Camenzind

November 3, 2002

Abstract

Quasars have been detected for the first time in the golden 60es of Astronomy, together with Radio Pulsars, the Cosmic Microwave Background and Gamma-Ray Bursters. In the past 30 years, the Black Hole paradigm for the explanation of the Quasar as high activity of the centers of galaxies has been confirmed. Since Quasars represent the exhaustive life of the center of a galaxy, their remnants can only grow in mass. This fact has been largely confirmed thanks to observations of high spatial resolution in the local Universe. Radio galaxies represent a particular activity where a large fraction of the central energy is converted into kinetic motion of plasma beams. The interaction of these plasma flows with the ambient cluster gas leads to X-ray and atomic line radiation and provides important insight into the structure of young galaxy clusters in the Early Universe. The question of the very origin of Quasars is at the forefront of the actual research.

The following topics will be covered:

- Active Quasars – the phenomenon, taxonomy, global spectra, redshift distribution, host galaxies and standard models;
- Quasar Remnants – Black Holes in the centers of galaxies as their remnants in the local Universe;
- Friedmanology – Cosmology for Quasars;
- Rotating Black Holes – Gravitational forces, frame-dragging, particle motion, ray-tracing, magnetospheres;
- Micro-Jets – Quasar jets and Radio Galaxies at low and high redshifts;
- Macro-Jets – Structure of radio galaxies and quasars, bow shocks, beams and hot spots, jets on the computer;
- Early Quasars – from the first stars at redshift 25 to Quasars.

*Lecture given in Heidelberg WS 2002/2003.

Contents

1	Quasars as Cosmological Objects	5
1.1	Basic Properties and a brief Historical Perspective	5
1.1.1	Seyfert Galaxies – the pre–Quasar Era	7
1.1.2	Radio Galaxies open up the Quasar–Era	10
1.1.3	Radio Surveys and Quasars – the Quasar Era	10
1.2	Modern Optical Surveys and Future IR – the post–Quasar Era	17
1.3	Global Spectra	19
1.3.1	Optical–UV Continuum	21
1.3.2	Infrared Emission	23
1.3.3	X–Rays	23
1.3.4	Gamma Rays	23
1.4	Quasar Models	30

List of Figures

1	Optical spectrum of NGC 1275	8
2	UV spectrum of NGC 5548	9
3	Composite image of Cygnus A	11
4	VLT image of M 87	12
5	Radio structure of M 87	13
6	HST image of 3C 273	14
7	Multi–wavelength view of the jet in 3C 273	15
8	Redshift of 3C 273	16
9	A 2dF Quasar with redshift 2.41	18
10	Redshift distribution of 2dF Quasars	19
11	NGST spectrum for high redshift Quasar	20
12	SED of Quasars	21
13	UV Spectra	22
14	ISO SED for PG quasars	24
15	ISO SED for PG quasars	25
16	Spectral slope for X–ray Quasars	26
17	Relativistic Fe lines	27
18	Gamma–ray sky	28
19	Spectrum of Mkr 421	29
20	Urry–Padovani cartoon	31
21	The Camenzind torus model for Quasars	33
22	Type II Quasar	34
23	SED for bright Quasars	35
24	Falcke model for jet sources	37

References

- [1] Peterson, B.M.: 1997, **An Introduction to active galactic nuclei**, Cambridge University Press (a very suitable introduction into the field of thermal Quasars)
- [2] Krolik, J.H.: 1998, **Active Galactic Nuclei: From the Central Black Hole to the Galactic Environment**, Princeton University Press (a modern Overview for all aspects)
- [3] Robson, I.: 1996, **Active Galactic Nuclei**, Praxis Publishing
- [4] Camenzind, M.: 1997, **Les noyaux actifs de galaxies**, Lecture Notes in Physics **m46**, Springer-Verlag (Heidelberg)
- [5] Rich, J.: 2001, **Fundamentals of Cosmology**, Springer-Verlag (Heidelberg)

1 Quasars as Cosmological Objects

Our understanding of the Quasar phenomenon is still in a primitive state after over 30 years of intense research in this area. Only in the last ten years, a global concept is emerging – quasars are just normal galactic nuclei, except for their tremendous fuelling rates. Quasars are typically found at redshifts from 0.3 to 3.0, but also at redshifts beyond 5. Whether they occur beyond redshift 6.5 can only be decided in future infrared observations. Quasars are therefore cosmological objects, and the underlying cosmological model is not unimportant for the understanding of the Quasar phenomenon. Accretion from the parsec-scale region in the core of a galaxy towards a supermassive Black Hole is the main driver of the observed activity. In the last ten years, important progress has been achieved in understanding this scenario by means of mass determinations for the central Black Holes. Mass and accretion rate are the two main parameters for the models. Quasars are only the tip of the iceberg of active galactic nuclei, since UV-emission disappears when the relative accretion rate decreases below a value of a few percent of the Eddington accretion rate. This is another fact we have learnt in the last few years.

1.1 Basic Properties and a brief Historical Perspective

In general the term **active galactic nucleus**, or AGN, refers to the existence of energetic phenomena in the nuclei, or central regions, of galaxies which cannot be attributed clearly and directly to stars. The two largest subclasses of AGNs are **Seyfert galaxies and quasars**, and the distinction between them is to some degree a matter of semantics. The fundamental difference between these two subclasses is in the amount of radiation emitted by the compact central source; in the case of a typical Seyfert galaxy, the total energy emitted by the nuclear source at visible wavelengths is comparable to the energy emitted by all of the stars in the galaxy (i.e. $\simeq 10^{11} L_{\odot}$), but in a typical quasar the nuclear source is brighter than the stars by a factor of 100 or more. Historically, the early failure to realize that Seyferts and quasars are probably related has to do with the different methods by which these two types of objects were first isolated, which left a large gap in luminosity between them. The appearance of quasars did not initially suggest identification with galaxies, which is a consequence of the basic fact that high-luminosity objects, like bright quasars, are rare. One is likely to find rare objects only at great distances, which is of course what happens with quasars. At very large distances, only the star-like nuclear source is seen in a quasar, and the light from the surrounding galaxy, because of its small angular size and relative faintness, is lost in the glare of the nucleus. Hence, the source looks *quasi-stellar*.

A brief history of detections:

- **1943:** American Astronomer Karl Seyfert undertakes a study of spiral galaxies with star-like nuclei and strong emission lines in their spectra. These objects are now called Seyfert galaxies.
- **1950:** Australian radio astronomer John Bolton discovers the cosmic radio sources Cygnus A, Virgo A and Centaurus A, and identifies them as galaxies.
- **1960:** English radio astronomers complete the 3rd Cambridge Catalog (known now as 3C Catalog), listing the brightness and positions of a few hundred cosmic radio sources, designated with a label 3C... Many of these galaxies are coincident with distant galaxies. The optical identification of practically all the sources has been completed in 1992 (Stickel et al. 1992).
- **1963:** Maarten Schmidt, working on the 5-m telescope on Mt. Palomar, studies the spectrum of 3C 273, a compact radio source with a starlike optical counterpart. He recognizes that the strong emission lines in this object are hydrogen lines redshifted by 16%, making 3C 273 the most distant object in the Universe known at that time. Soon afterwards, astronomers discover another quasar, 3C 48, with a redshift of 37%.
- **1960s–1970s:** Astronomers discover hundreds of quasars, radio galaxies, and other active galaxies. They find that many of these sources vary in brightness on timescales from days to years.
- **1978:** NASA launches the Einstein Observatory, the first imaging X-ray satellite. They find that virtually all Seyfert galaxies and a few quasars are luminous X-ray sources.
- **1980s:** Radio astronomers, working with the VLA and MERLIN telescope in England, map the radio emission from hundreds of radio galaxies and quasars. They find that the radio sources typically have jets emanating from a compact nucleus and terminating in lobes of radio emission far beyond the optical galaxy.
- **1990s:** NASA's new Compton Gamma Ray Observatory observes that some quasars and active galaxies are powerful sources of high energy gamma rays that vary in timescales of days. These objects are usually called Blazars.
- **1995:** Radio astronomers from Harvard and Japan use very long baseline interferometry (VLBI) to measure the rotation velocities of radio emission lines from the very bright water masers in molecular clouds near the nucleus of the Seyfert galaxy NGC 4258 and find that these clouds are orbiting a black hole with mass of 35 million solar masses.

- **2001:** Discovery of the quasar with highest redshift 6.25 in the Sloan Digital Sky Survey (SDSS). SDSS will add about 100'000 new Quasars to the catalogs. The 2dF survey in Australia has already detected about 23'000 Quasars in small strips.
- **2002:** Today, astronomers have discovered more than 30'000 of quasars, and especially some with redshift greater than 5. Only about 10% of these are luminous radio sources. Astronomers have found the remnants of the quasar activity in the form of supermassive black holes in many nuclei of nearby galaxies, including our own one.
- **> 2002:** INTEGRAL, XMM–Newton and Chandra will explore the X–ray and gamma–emission of Quasars. SIRTf may give some clue to the infrared spectrum of these objects.

1.1.1 Seyfert Galaxies – the pre–Quasar Era

The first optical spectrum of an active galaxy was obtained at Lick Observatory by E.A. Fath in 1908 as part of his dissertation work. He noted the presence of strong emission lines in the nebula NGC 1068. V.M. Slipher at Lowell Observatory obtained a higher-quality, higher-resolution spectrum of NGC 1068, and commented that the emission lines are similar to those seen in planetary nebulae. He also made the important observation that these lines are resolved, and have widths of hundreds of kilometers per second. Carl Seyfert (1943) was the first to realize that there are several similar galaxies which form a distinct class. Seyfert selected a group of galaxies on the basis of high central surface brightness, i.e., stellar-appearing cores. Seyfert obtained spectra of these galaxies and found that the optical spectra of several of these galaxies (NGC 1068, NGC 1275 1, NGC 3516, NGC 4051, NGC 4151, and NGC 7469) are dominated by high-excitation nuclear emission lines (Figs. 1 and ??). The important characteristics of these spectra were found to be:

- The lines are broad (up to 8500 km/s, full width at zero intensity).
- The hydrogen lines sometimes are broader than the other lines.

Seyfert galaxies received no further attention until 1955, when NGC 1068 and NGC 1275 were detected as radio sources. Woltjer (1959) made the first attempt to understand the physics of Seyfert galaxies. He noted the following:

The nuclei are unresolved, so the size of the nucleus is less than 100 pc. The nuclear emission must last more than 10^8 years, because Seyfert galaxies constitute about 1 in 100 spiral galaxies.

This is a simple argument. One extreme scenario is that galaxies which are Seyferts are always Seyferts, in which case their lifetime is the age of the Universe (10^{10}

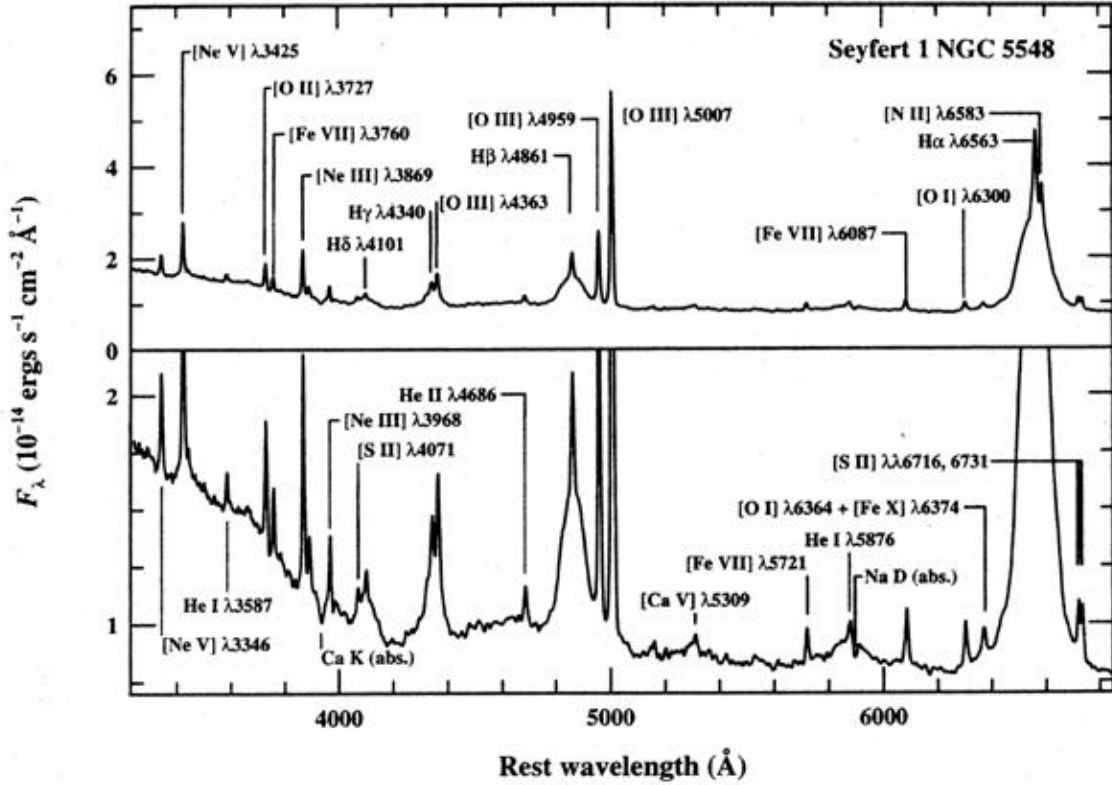


Figure 1: The optical spectrum of the Seyfert 1 galaxy NGC 1275. The prominent broad and narrow emission lines are labeled, as are strong absorption features of the host galaxy spectrum. The vertical scale is expanded in the lower panel to show the weaker features. The full width at half maximum (FWHM) of the broad components is about 5900 km s^{-1} , and the width of the narrow components is about 400 km s^{-1} . The strong rise shortward of 4000 \AA is the long-wavelength end of the *small blue bump* feature which is a blend of Balmer continuum and FeII line emission. This spectrum is the mean of several observations made during 1993 with the 3-m Shane Telescope and Kast spectrograph at the Lick Observatory. Data courtesy of A. V. Filippenko.

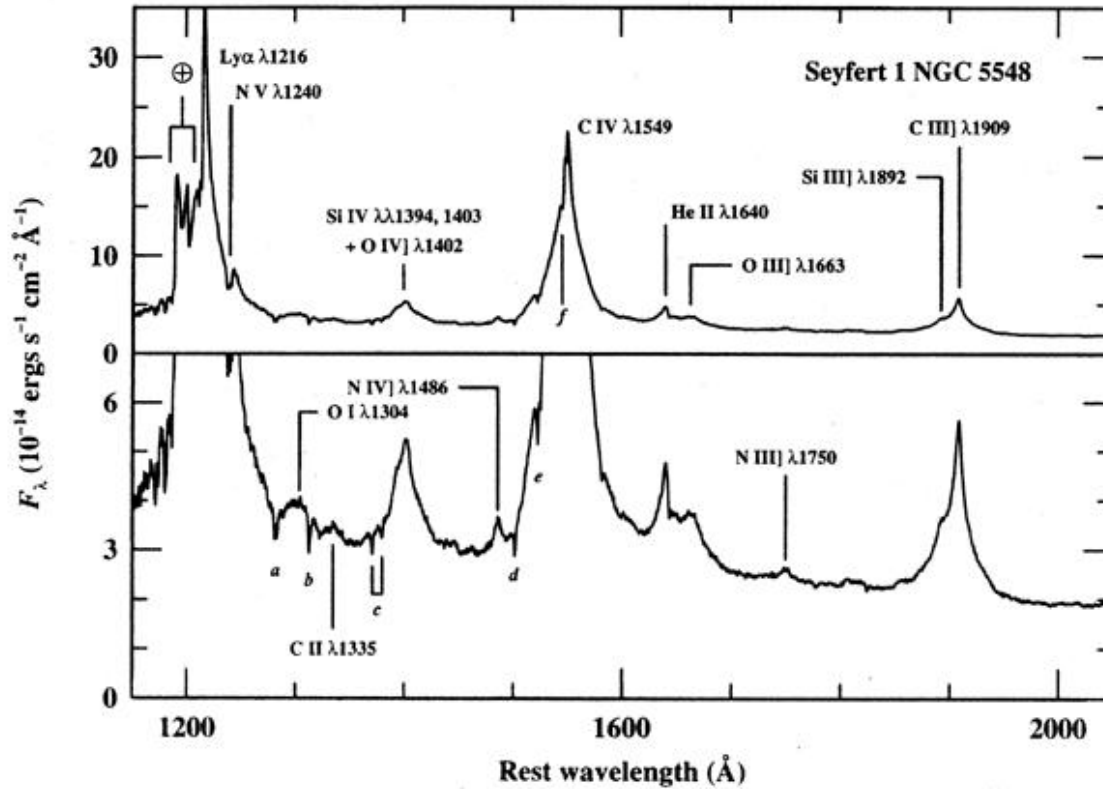


Figure 2: The ultraviolet spectrum of the Seyfert 1 galaxy NGC 5548. The prominent broad emission lines are labeled. The emission labeled with the Earth symbol arises in the extended upper atmosphere of the Earth and is known as *geocoronal* emission. Most of the labeled absorption features arise in our own Galaxy and thus appear blueshifted from their rest wavelengths since the spectrum has been corrected for the redshift of NGC 5548 ($z = 0.017$). The labeled absorption features are O II 1302 (a), C II 1335 (b), Si IV 1394, 1403 (c), Si II 1527 (d), and C IV 1548, 1551 (e). Another weak C IV 1548, 1551 doublet (f) is only slightly displaced shortward of line center and presumably arises in NGC 5548 itself. This spectrum is the mean of several observations obtained with the Faint Object Spectrograph on the Hubble Space Telescope in 1993. Data courtesy of K. T. Korista.

years). The opposite extreme is one where all spirals pass through a Seyfert phase (or phases) - since 1 spiral in 100 is currently in the Seyfert phase, it must last of order $10^{10}/100 = 10^8$ years.

1.1.2 Radio Galaxies open up the Quasar–Era

In the early 1960s, radio astronomers from England completed the third Cambridge Catalog of radio sources. They found that many of these radio sources were coincident with distant galaxies. With the much better angular resolution of VLA and VLBA radio telescope arrays, one can see that these radio sources often consist of point sources at the center of the galaxy and extended sources that extend thousands or even millions of light years beyond the galaxy into the intergalactic space. Cygnus A is still one of the brightest radio source in the sky and the classical example of a double–lobed radio galaxy. The radio emission comes primarily from two giant radio lobes in intergalactic space, each displaced 70 kpc from the central galaxy (the tiny spot in the center of the image). One also can see faint jets of radio emission extending from this central point to both lobes. At the bright radio lobes the beams are stopped by collisions with the intergalactic gas.

The jets in radio galaxies might remind us of the jets seen in star–forming regions. But they are very different. The jets in star–forming regions are expanding with velocities of a few hundred km/s, while the jets from radio galaxies are expanding at nearly the speed of light (300,000 km/s). The jets in star–forming regions only extend a few light years, while those in radio galaxies can extend to a few hundred kpc or even Mpc. They have however in common that both are produced when gas accretes onto a central object.

Besides emission line objects, a strange linear feature has already been detected in 1913 for the elliptical galaxy M 87 (Curtis 1913, Fig. 4). Due to its linear structure it has been called **Jet**. The optical emission from this feature is highly polarized synchrotron emission which is also visible in the radio domain (Fig. 5).

1.1.3 Radio Surveys and Quasars – the Quasar Era

Quasars were originally discovered as a result of the first radio surveys of the sky in the late 1950s. By this time, the angular resolution of radio observations was good enough to identify the strongest radio sources with individual optical objects, often galaxies, but sometimes stellar–appearing sources. Important early surveys included the following:

- **3C and 3CR:** The third Cambridge (3C) catalog (Edge et al. 1959), based on observations at 158 MHz, and its revision, the 3CR catalog (Bennett 1962), at 178 MHz, detected sources down to a limiting flux of 9 Jy 1. The 3C catalog is not limited by flux sensitivity, but by *confusion* of sources at low flux levels; fainter sources become so numerous on the sky that they cannot

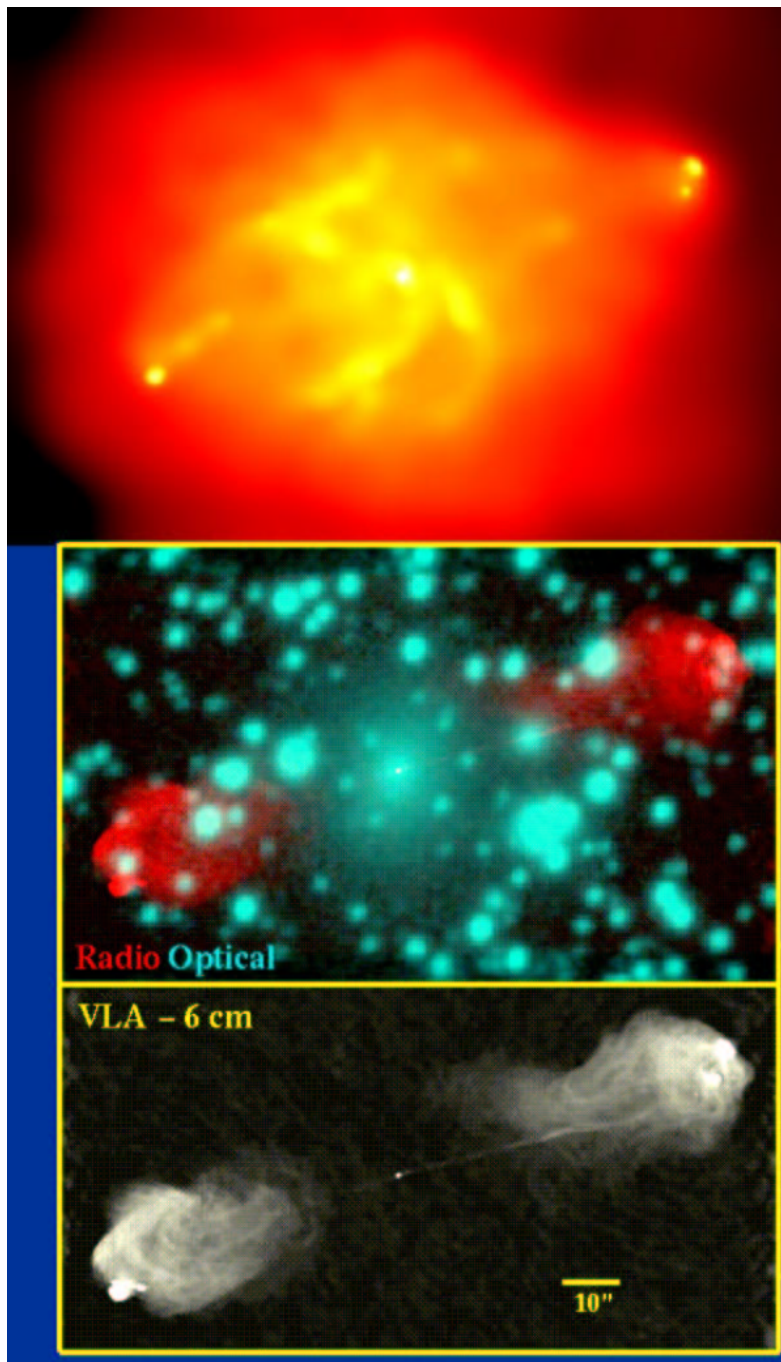


Figure 3: A composite image of Cygnus A: X-rays (top, Chandra), optical image with radio lobes as overlay(middle panel) and VLA at 6 cm (bottom panel) which shows the central point source identical with the center of the optical galaxy, the two beams, hot spots and radio lobes.

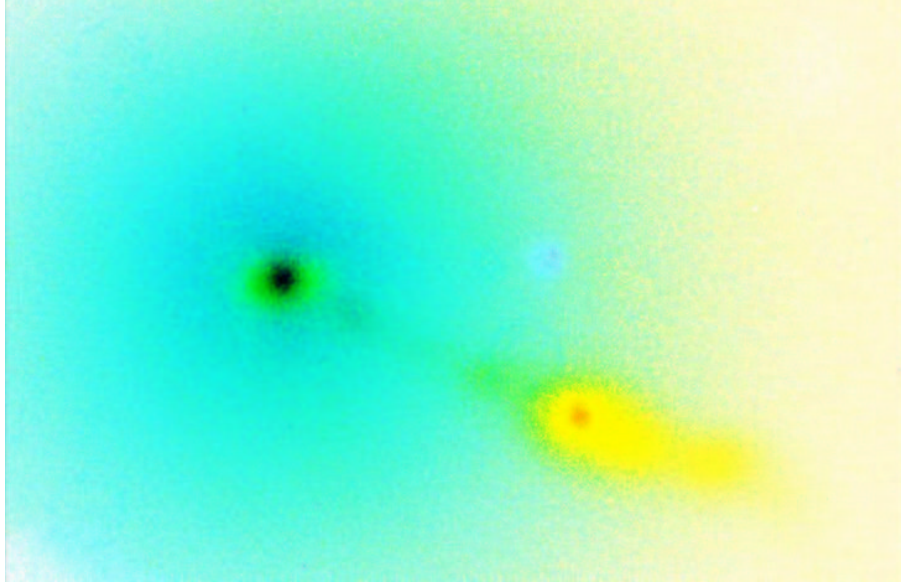


Figure 4: VLT image of Messier 87 with its stellar core and jet, already detected by Curtis in 1913. The stellar core has a radial extension of about 660 pc. The projected size of the jet is about 2 kpc.

be unambiguously distinguished from one another with poor angular resolution observations. There are 471 3C sources, and 328 3CR sources, numbered sequentially by right ascension (e.g., 3C 273, which is at epoch 1950.0 coordinates $1950 = 12^{\text{h}} 26^{\text{m}} 33.^{\text{s}}35$, $1950 = +0219'42''$), with the numbering between the two catalogs kept as consistent as possible. Sources which appear in the 3CR but not the 3C are kept in proper right ascension order by appending a decimal point and additional digit to the immediately preceding source (e.g., 3C 390.3). All 3C sources are north of -22 declination, but the 3CR excludes sources south of -5 .

- **PKS:** This was an extensive survey (Ekers 1969) of the southern sky (declination $< +25$) undertaken at Parkes (PKS), Australia, originally at 408 MHz (detection limit 4 Jy) and later at 1410 MHz (to 1 Jy) and 2650 MHz (to 0.3 Jy). These sources are designated by 1950.0 position, using the format “HHMM \pm DDT”, where HHMM refers to the hours and minutes of right ascension (epoch 1950.0), \pm is the sign of the declination, and DDT is the declination, in degrees (DD) and tenths (T) of degree 2 (e.g., 3C 273 = PKS 1226+023); this is still the most common, and useful, system of naming quasars.
- **4C:** The Fourth Cambridge survey was a more sensitive version (limiting flux 2 Jy) of the 3C, again undertaken at 178 MHz (Pilkington and Scott 1965, Gower, Scott, and Wills 1967). Names of 4C sources are given as “DD.NN”,

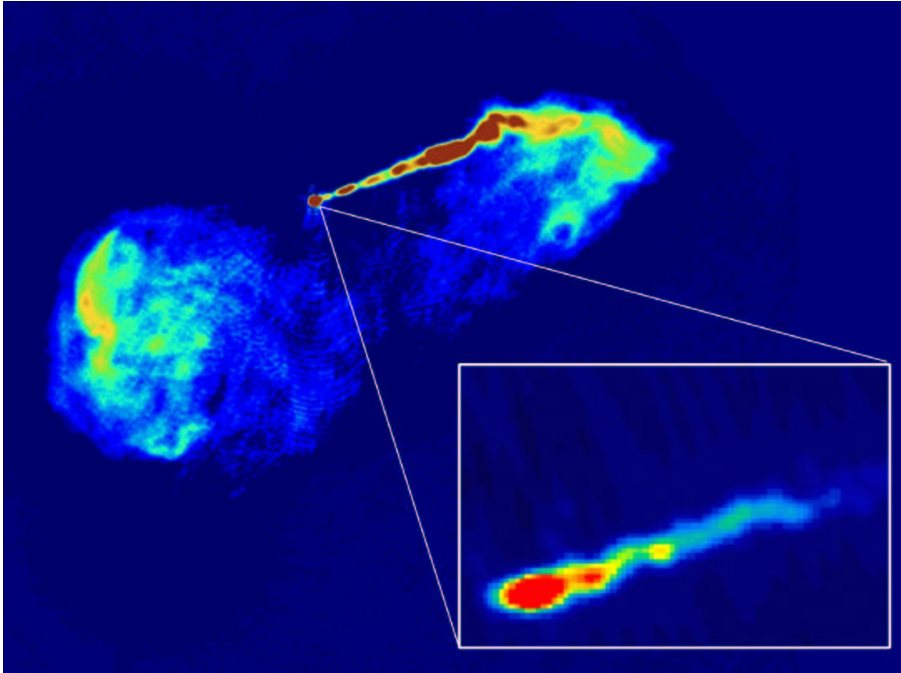


Figure 5: The radio structure of M87 from VLA (top) and VSOP (bottom, small-scale jet).

where DD is the source declination, and NN is a sequence number within the declination band (e.g., 3C 273 = 4C 02.32).

- **AO:** The Arecibo Occultation (AO) survey is notable for the extremely accurate positions it produced as a result of observing radio sources as they were occulted by the Moon (Hazard, Gulkis, and Bray 1967). As a small angular size radio source is occulted by the Moon, the moment of disappearance identifies its position as being somewhere along the locus of points defined by the preceding limb of the Moon. Subsequent occultations of the same source give additional such loci, all of which intersect at a single point. Thus, the location of the points is limited by timing accuracy and the accuracy to which the position of the limb of the Moon is known, not by the size of the radio beam. Names of these sources are Parkes-style.
- **Ohio:** The Ohio radio survey (e.g., Ehman, Dixon, and Kraus 1970) was made with a unique 79 x 21m transit telescope at 1415 MHz. The unusual geometry of the telescope produces an irregular beam of half-power beam width $10'$ in right ascension and $40'$ in declination. Source names are given as “Ox-NNN”, where x is a letter indicating an hour-wide band of right ascension (with “A” and “O” excluded 3, so sources between 0h and 1h are “OB” and sources between 23h and 0h are “OZ”) and NNN is a serial number (e.g., 3C 273 = ON 044). As in many of the early surveys, the positions and fluxes

are not reliable (particularly at sub-jansky flux levels), but the Ohio survey is notable in that up through the late 1970s some of the most distant and most luminous known quasars (e.g., OQ 172 = 1442+101 and OH 471 = 0642+449) were Ohio sources.

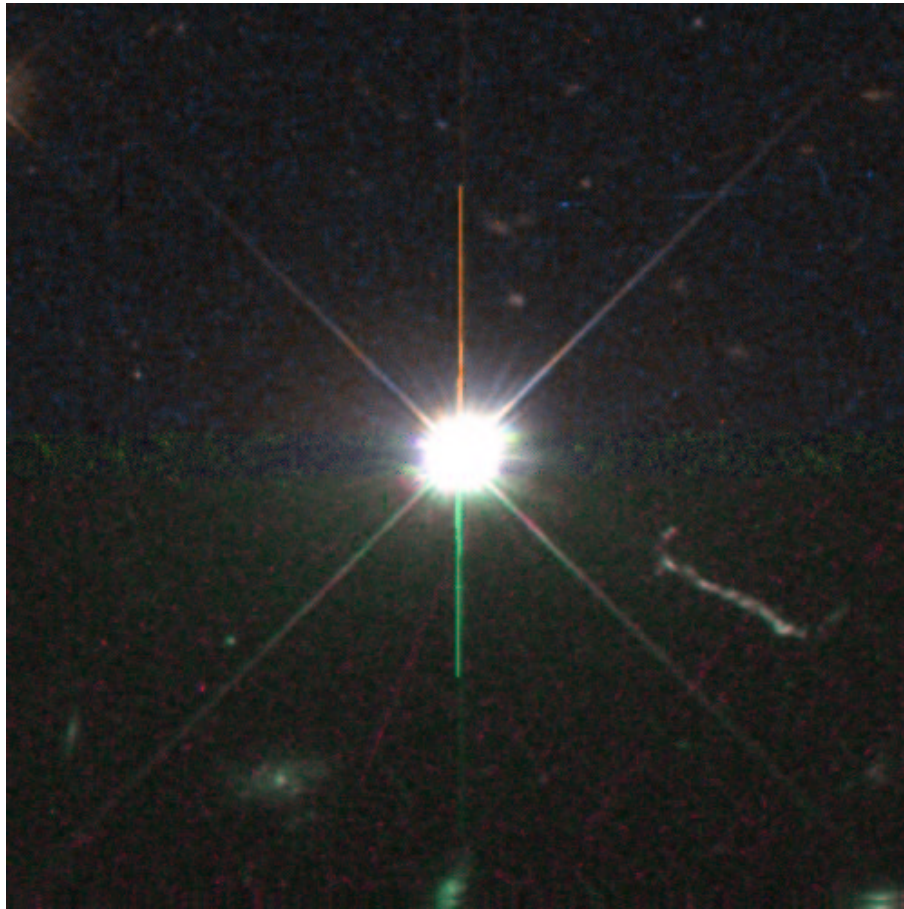


Figure 6: HST image of 3C 273 with its jet.

Most radio sources at high Galactic latitude were identified with resolved galaxies. However, the positions of some of these radio sources were found to be coincident with objects that looked like stars on normal photographs, such as the Palomar Sky Survey. The first strong radio source unambiguously identified with a star-like optical source was 3C 48. On the basis of a radio position obtained with a two-element interferometer, Matthews and Sandage (1963) found that the optical counterpart of this source was a magnitude 16 star. However, the photographic spectra obtained of this source were very confusing, as they showed strong very broad emission lines at unidentified wavelengths. It is worth noting how unsuitable photographic spectra are for work on quasars; it was unclear to the first investigators whether these broad features were emission lines or merely the continuum between broad absorption lines, as in white dwarf spectra. Photometry of these objects revealed that they

are anomalously blue (relative to normal stars). Needless to say, the nature of these “radio stars” was very uncertain.

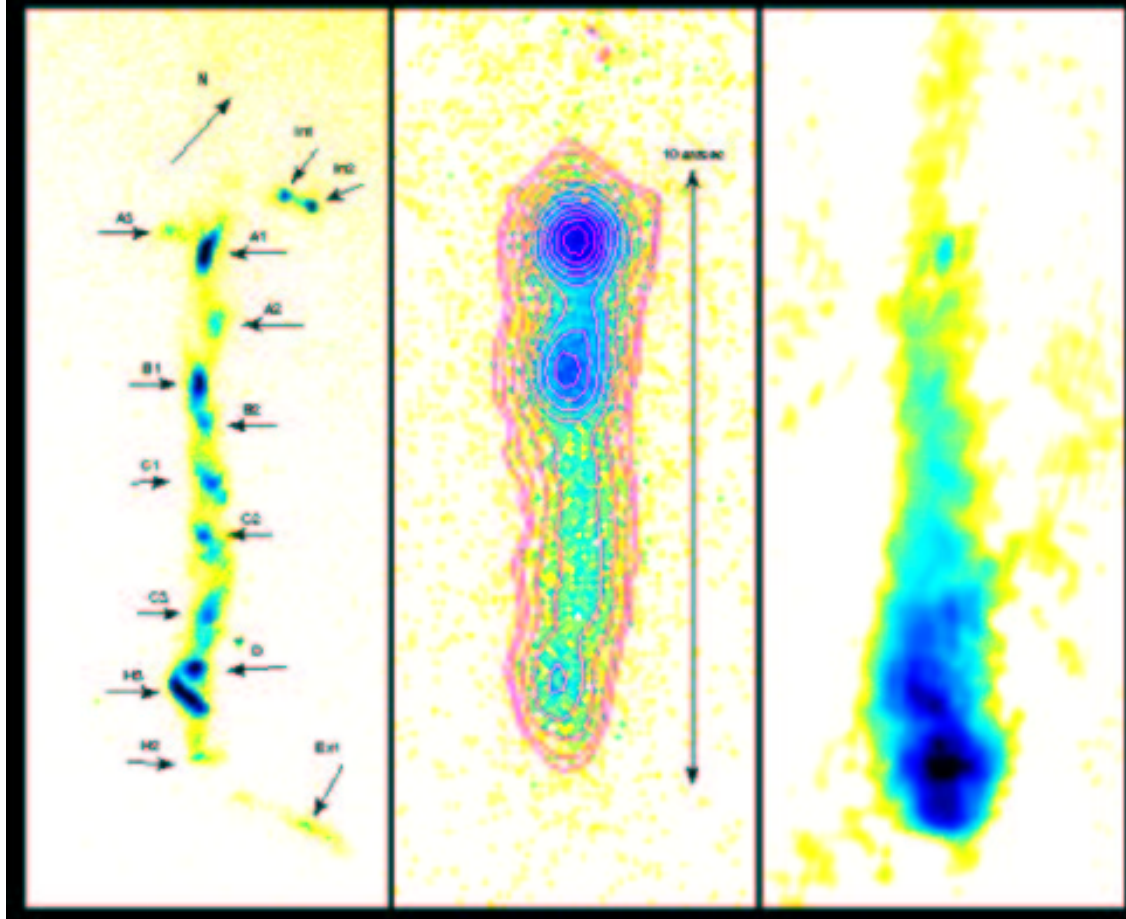


Figure 7: A modern view of the jet in 3C 273 in the optical (left), X-rays (middle) and radio (right). The jet is rotated, the Quasar is beyond the upper edge of the figure, the first knot occurs at a distance of 12 arcsec from the Quasar. Optical and radio emission is synchrotron emission by highly relativistic electrons, X-rays are generated by inverse Compton scattering on the microwave background radiation.

Another radio source identified with a star-like object, in this case on the basis of an accurate lunar occultation measurement (Hazard, Mackey, and Shimmins 1963), was 3C 273. The first breakthrough in understanding these extraordinary objects came with Maarten Schmidt’s realization (Schmidt 1963) that the emission lines seen in the spectrum of this source were actually the hydrogen Balmer-series emission lines and Mg II 2798 at the uncommonly large redshift $z = 0.158$, where we recall that the redshift is an observational quantity defined by the observed wavelength λ_O of a spectral line relative to its laboratory wavelength λ_E ,

$$z = \frac{\lambda_O - \lambda_E}{\lambda_E} \quad (1)$$

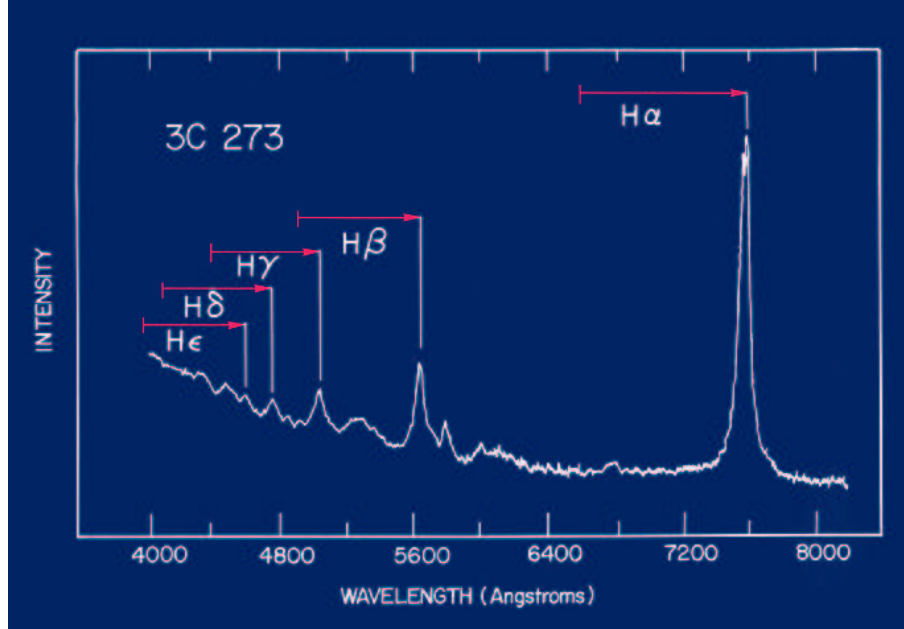


Figure 8: Redshifted emission lines of 3C 273

This redshift was approximately an order of magnitude larger than those of the original Seyfert galaxies and was among the largest ever measured at the time, with only a few very faint rich clusters of galaxies rivaling it. The obvious interpretation of the redshift is that it is of cosmological origin, a consequence of the expansion of the Universe, and the Hubble law thus gives the distance

$$d = \frac{cz}{H_0} = 3000 h^{-1} z \text{ Mpc} \quad (2)$$

where h is the Hubble constant in units of $100 \text{ km s}^{-1} \text{ Mpc}^{-1}$. More disturbing than this vast distance was the enormous luminosity implied; 3C 273 was and remains the brightest known quasar ($B = 13.1 \text{ mag}$). Using the formula for the distance modulus

$$m - M = 5 \log(cz/H_0) + 25 \quad (3)$$

(where cz/H_0 is measured in Mpc), the absolute magnitude of 3C 273 is $M_B = -25.3 + 5 \log h$, which is about 100 times as luminous as normal bright spirals like the Milky Way or M31. Once the redshift mystery was unlocked, identification of lines in 3C 48 (Greenstein and Matthews 1963) and other quasar spectra followed quickly.

As the physical nature of these luminous star-like objects was not understood, they became known simply as **quasi-stellar radio sources**, a term which was subsequently shortened to **quasars**.

The probable importance of quasars was recognized immediately. The extremely high luminosities of these objects implied physical extremes that were not found elsewhere in the nearby Universe. The suggestion that massive black holes might be

involved appeared early (e.g., Zel’dovich and Novikov 1964). The possible role of active nuclei in galaxy formation and evolution was also seen (e.g., Burbidge, Burbidge, and Sandage 1963). The high luminosities of quasars also imply that they might serve as important cosmological probes, since they could be in principle detected and identified at very large distances. These considerations provided early and continuing strong motivation for finding quasars and studying their properties. As the number of known quasars increased, progressively greater and greater redshifts were identified, and as of the mid-1990s the highest observed redshifts are $z \simeq 5$. In the meantime, redshifts beyond 6.0 have been found.

If the material in the nucleus is gravitationally bound, the mass of the nucleus must be very high. This is a simple virial argument, i.e.,

$$M \simeq R \sigma^2 / G \quad (4)$$

The velocity dispersion σ is obtained from the widths of the emission lines and is of order 10^3 km/s. We have an upper limit to the size of the nucleus ($R < 100$ pc) from the fact that it is spatially unresolved. The emission lines are characteristic of a low-density gas, which effectively provides a lower limit $R < 1$ pc. Thus the mass of the nucleus can be inferred to be in the range $M \simeq 10^{8 \pm 1} M_{\odot}$.

This point tells us that something very extraordinary is occurring at the centers of Seyfert galaxies. If a large value of R is assumed, then it must be concluded that something like 10% of the mass of the galaxy is contained in a volume $\simeq 100$ pc across. On the other hand, if R is much smaller than the upper limit set by ground-based spatial resolution, then the problem to be faced is how to generate an extraordinary amount of energy in a tiny volume.

1.2 Modern Optical Surveys and Future IR – the post–Quasar Era

The problems inherent in the detection of significant numbers of quasars have long since been overcome. The fourth Hewitt and Burbidge catalog (Hewitt and Burbidge 1993) lists positions, magnitudes and redshifts for 7315 quasars. This and the earlier versions of the catalog (Burbidge, Crowne and Smith 1977, Hewitt and Burbidge 1980, 1987), together with the catalog of Veron–Cetty and Veron (1991) and references therein, have proven to be an invaluable resource, but by their nature consist of an extraordinarily heterogeneous mix. Focusing more particularly on samples suitable for statistical analyses of the quasar population, Boyle (1993) has provided a graphic illustration of the pace of change. He plots absolute magnitude versus redshift to illustrate the growth of the number of objects published in well-defined surveys for quasars in the optical passbands. The number of objects in such samples has grown exponentially in recent years, with an attendant significant increase in our knowledge of how the quasar population evolves with cosmic time. However, given the large numbers of quasars now cataloged, the lack of even qualitative answers to basic questions, such as *Do the spectral energy distributions of*

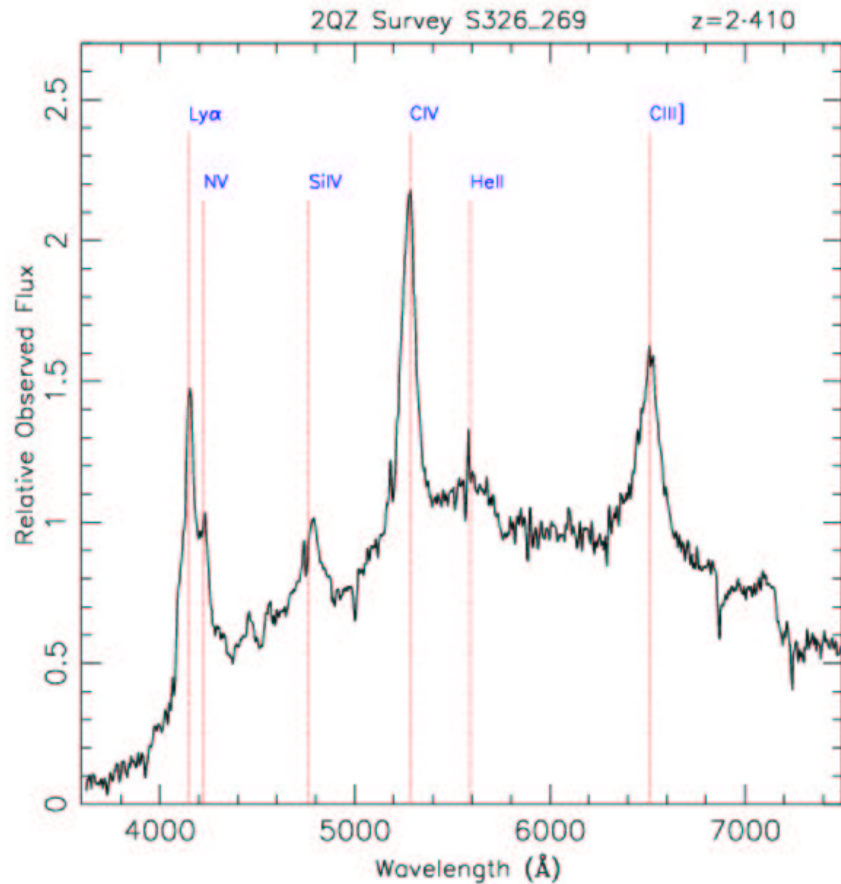


Figure 9: Spectrum of a 2dF Quasar with redshift 2.41.

quasars evolve as a function of cosmic time? or, Does the space density of quasars decline at redshifts $z > 4$? appears surprising.

Quasars are nowadays searched for in large optical surveys (2dF in Australia and SDSS in the States, with participation of the MPI for Astronomy in Heidelberg). In the past, various survey techniques have been applied (see Peterson 1997). The COMBO-17 survey (MPIA Heidelberg) has imaged 1 square degree of sky in 17 optical filters using the Wide Field Imager at the MPG/ESO 2.2-m telescope on La Silla. The multi-color spectra are resolved well enough to classify 50.000 objects at $I < 23$ into stars, galaxies and quasars as well as strange objects. Spectral subclassification and redshifts for galaxies and quasars are also obtained. A deep sharp R-band image allows morphological and lensing studies. Observations over two years allow variability studies at very faint levels.

Quasars with redshifts beyond 6.5 have to be searched for in the near IR (Fig. 11).

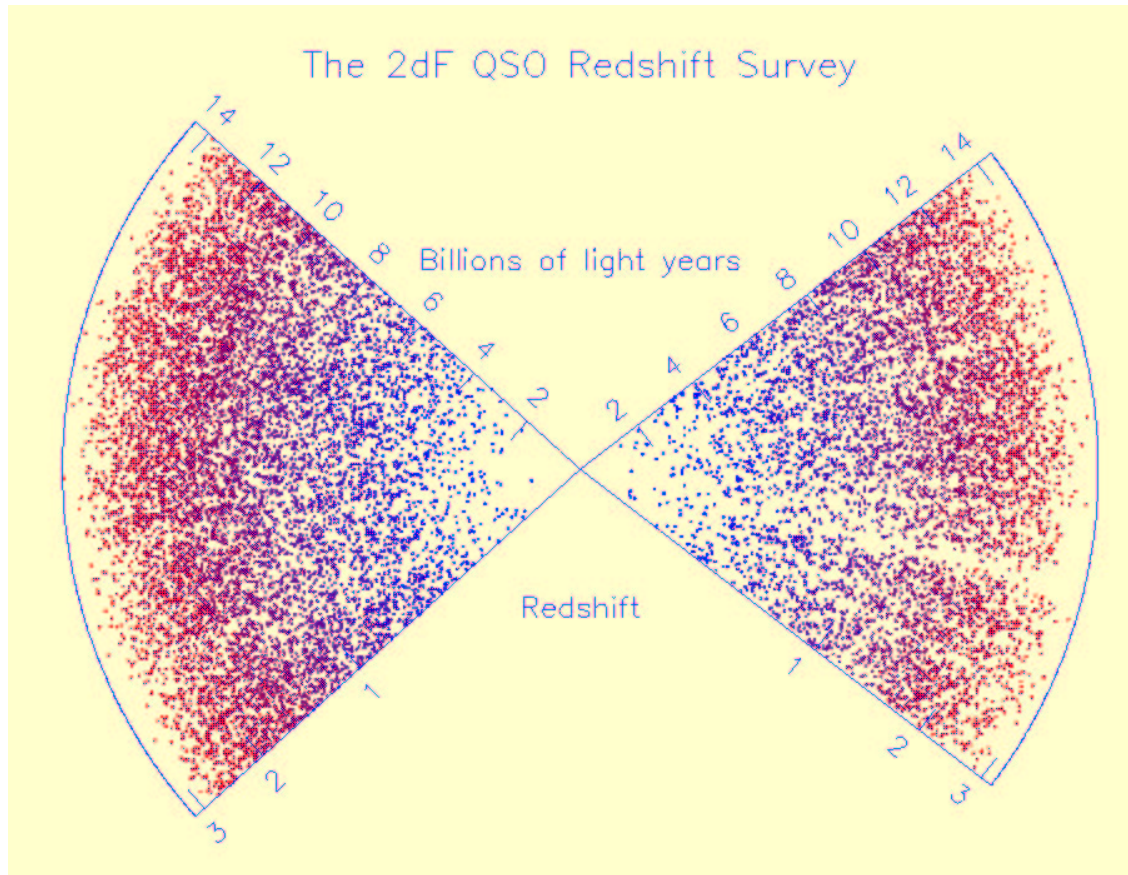


Figure 10: Distribution of 2dF Quasars in redshift or look-back time. It is quite evident that there are no local Quasars detected.

1.3 Global Spectra

Quasars exhibit significant emission in nearly all wavebands studied to date. Their spectra span hard X-rays to the far infrared with almost equal power per decade of frequency. Closer inspection reveals a number of features such as dips and bumps that consistently recur from one AGN to the next. These features are illustrated in Fig. 12 which is loosely based on the mean spectrum of a sample of predominantly ‘UV excess’ selected quasars from Elvis et al. (1994). The most notable features include the following:

- The **big blue bump** covers the wavelength range from 4000 to at least 1000 Å. Whether this feature extends further into the EUV is unclear. Our galaxy becomes virtually opaque at wavelengths between 912Å and $\simeq 100$ Å due to absorption by neutral hydrogen.
- The **near-infrared inflection** appears as a dip between 1.0 μm and 1.5 μm . This is practically the only continuum feature with a well defined wavelength (Neugebauer et al. 1987).

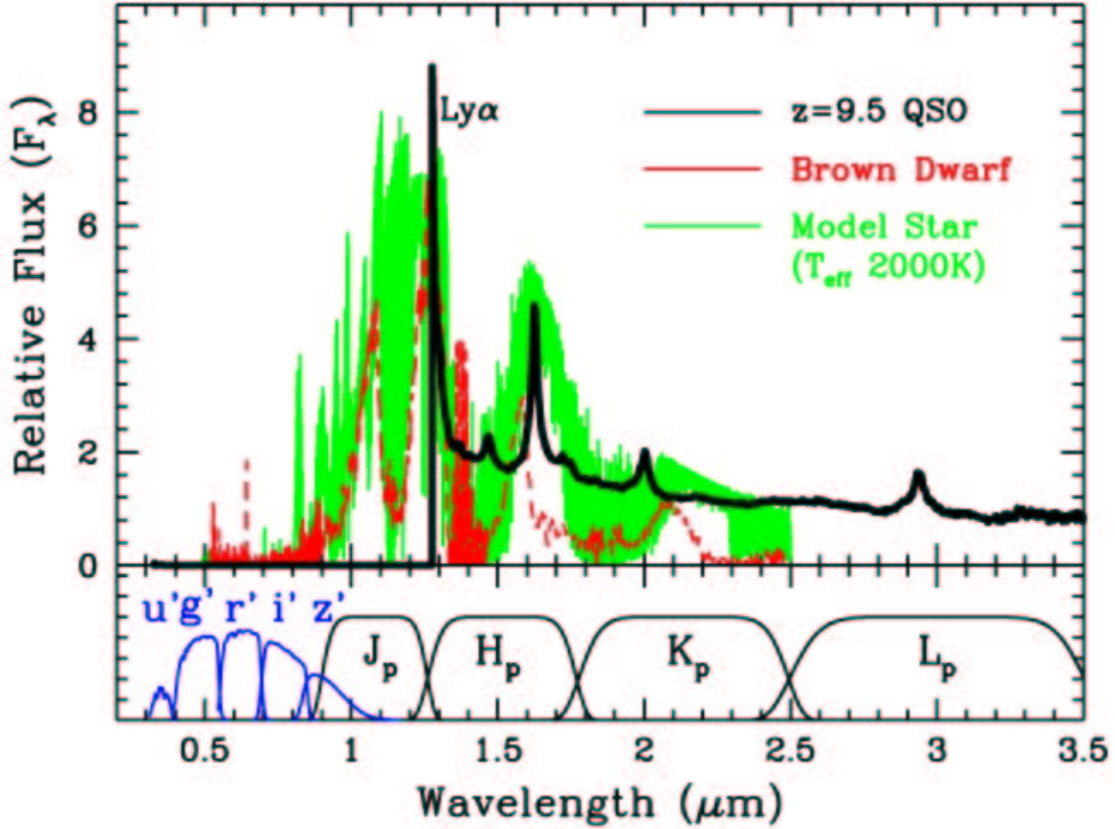


Figure 11: Spectrum of a putative quasar with extremely high redshift 9.5 in comparison with spectra of cool stellar objects. Blueward of $\text{Ly}\alpha$, all emission gets absorbed in the neutral hydrogen of the early Universe.

- The **infrared bump** is a broad feature longward of the $1 \mu\text{m}$ inflection. The ‘submillimetre break’ marks a sharp drop in emission and is the strongest feature seen in normal quasar continua. The exact location of this feature and the size of the drop varies within the AGN population. In ‘radio-loud’ objects the drop in power output is only about two decades, while for the more common ‘radio-quiet’ objects it may be about 5 or 6 decades (Elvis et al. 1994).
- The X-ray continuum can broadly be described as a power-law from energies of one keV up to an eventual cut-off somewhere beyond 100 keV.
- The **soft X-ray excess** describes an emission component observed below one keV. This appears to be a common feature of Seyfert galaxies (Pounds & Reeves 2002) and quasars (Elvis et al. 1994) though may not be ubiquitous.

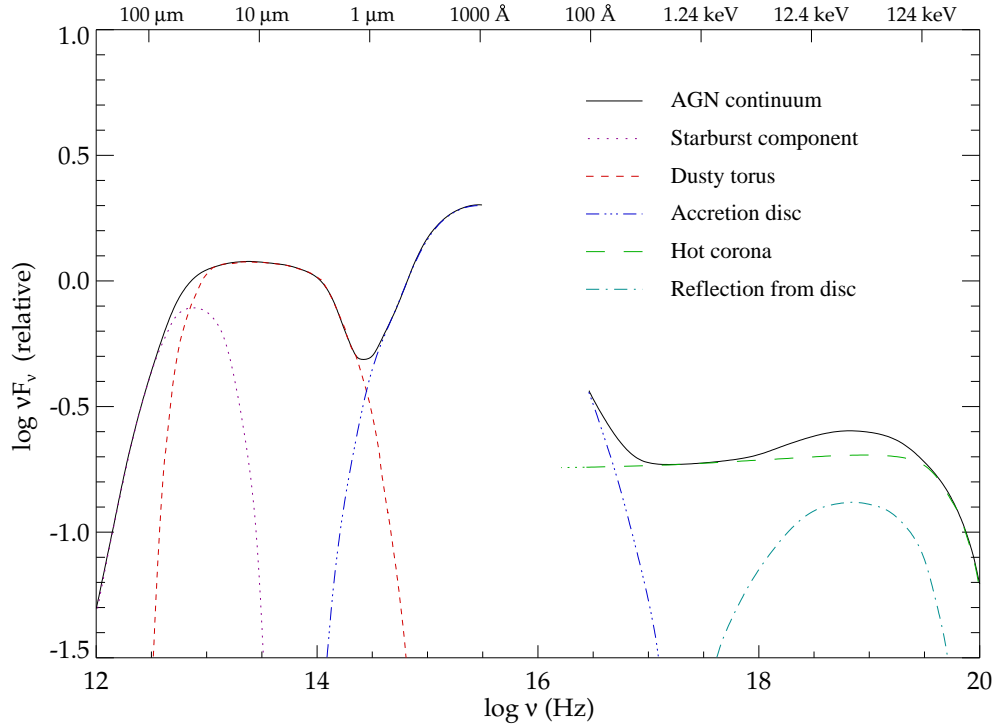


Figure 12: Global spectra of quasars. A typical quasar spectrum disposes of three different bumps in the spectral energy distribution: the UV–bump, the infrared bump and a hard X–ray contribution extending up to 120 keV.

1.3.1 Optical–UV Continuum

Dominating the optical–UV spectra of AGN is the broad continuum feature known as the **big blue bump**. The exact shape of this feature is confused by a large number of broad and blended lines thought to be emitted from fast moving ionised clouds near the centre of the AGN. In particular, superimposed on the continuum between 2000 and 4000 Å is a feature known as the ‘small blue bump’, made up of the Balmer continuum and blended Balmer and Fe II line emission. Figure ?? displays these features in a composite quasar spectrum. At wavelengths redward of Ly α the composite uses quasars from the Sloan Digital Sky Survey selected on the basis of their optical colours (Vanden Berk et al. 2001). The slope of the optical continuum generally varies between -1 to 0 , from Quasar to Quasar. For this sample the median slope is $\alpha_V = -0.46$. The continuum blueward of the Lyman edge is rarely observed. However Zheng et al. (1997), compiled a spectrum from a sample of redshift $z \simeq 1$ quasars with relatively low line-of-sight column densities for intergalactic absorption. The composite HST/FOS spectrum is displayed blueward of Ly α in Fig. 13. There appears to be a break in the continuum slope at 1050 Å with $\alpha \simeq -1.8$ in the far ultra-violet. It should be noted that there are a number of

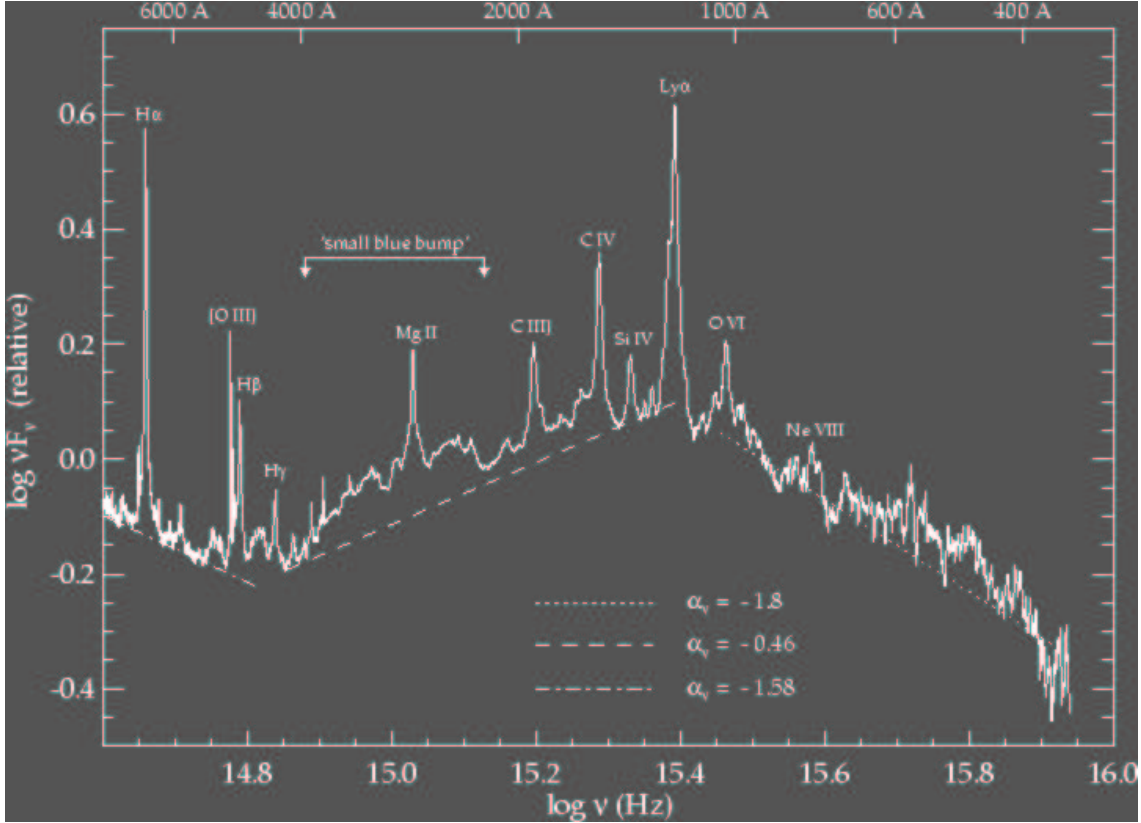


Figure 13: Optical–UV composite quasar spectrum. Longward of $\text{Ly}\alpha$, data is compiled from 2200 quasars from the Sloan Digital Sky Survey (Vanden Berk et al. 2001). The change in slope at 5000 \AA may be partly due to host-galaxy contamination. Shortward of $\text{Ly}\alpha$, data has been taken from HST/FOS observations of radio quiet quasars, corrected for Galactic reddening and intergalactic absorption (Zheng et al. 1997).

difficulties in measuring the true spectral slope in optical-UV data due to absorption and emission in intervening material. Host galaxy contamination can play a major role in low luminosity AGN, especially in the case of a nuclear starburst that can rarely be resolved. Intrinsic reddening by dust very close to the AGN can also have a dramatic effect on the slope of the observed spectrum. Problems also arise from combining spectra that may be from objects in intrinsically different states. Therefore, composite spectra, while useful for estimating the total output of the AGN population, do not have any real physical meaning. Models of the source emission need to be able to fit individual spectra.

Most current models interpret the big blue bump as thermal emission from an optically thick, geometrically thin accretion disc. A radial temperature distribution in the disc results in emission approximated by a multi-blackbody spectrum. Therefore, the majority of the flux at different wavelengths is emitted from physically

distant regions of the disc. This immediately causes a problem for these models as variations in the continuum are observed to be virtually simultaneous at optical and UV wavelengths (Ulrich et al. 1997). Changes would therefore need to propagate at speeds much greater than the sound speed in the optically thick medium. The multi-blackbody model also has problems fitting the optical continuum slope, usually producing spectra that are too ‘blue’ to fit the data.

More realistic models consider vertical structure and radiative transfer along the disc, often using stellar atmosphere models. However, these predict features that are generally not seen in Quasar ultra-violet spectra. The optical depth to bound-free absorption in the disc will change sharply at the Lyman limit (912 Å). Effectively, photons redward of the Lyman limit may escape from deeper regions of the disk. Therefore, if a temperature gradient is present there should be a Lyman edge in the UV spectrum. A rest-frame Lyman edge feature is rarely observed ($\simeq 10\%$ of cases, Koratkar & Blaes 1999) and in these is extremely weak. The models also predict electron scattering opacity to be important in the disc which would lead to significant polarisation in an orientation perpendicular to the disc axis. Observed optical polarisations are much lower than those predicted and appear to be parallel to the disc axis, where this can be inferred from radio jets (Kembhavi & Narlikar 1999).

1.3.2 Infrared Emission

A substantial fraction of the bolometric luminosity is emitted in infrared wavelengths [10] (Figs. 14, 15). Studies with ISOPHOT have confirmed that at least PG Quasars are strong infrared emitters.

1.3.3 X–Rays

An international team of scientists led by Penn State Associate Professor of Astronomy and Astrophysics Niel Brandt has used NASA’s Chandra X-Ray Observatory to detect the three most distant known quasars, among the most luminous objects in the Universe. The team’s observations with Chandra recorded high-energy X-ray emissions that were produced more than 10 billion years ago by the quasars’ massive black holes.

These three short Chandra observations provide the highest X–ray detection todate. There is no strong evolution

1.3.4 Gamma Rays

A few quasars turned out to be gamma ray sources. Fig. 18 is the Gamma Ray Sky as observed by the Compton Gamma Ray observatory operating from 1990 to 1999. The bright sources above and below the Milky Way are blazars, e.g. the brightest one is the blazar 3C 279. Its brightness can increase or decrease by factors of four within a few days (Fig. ??).

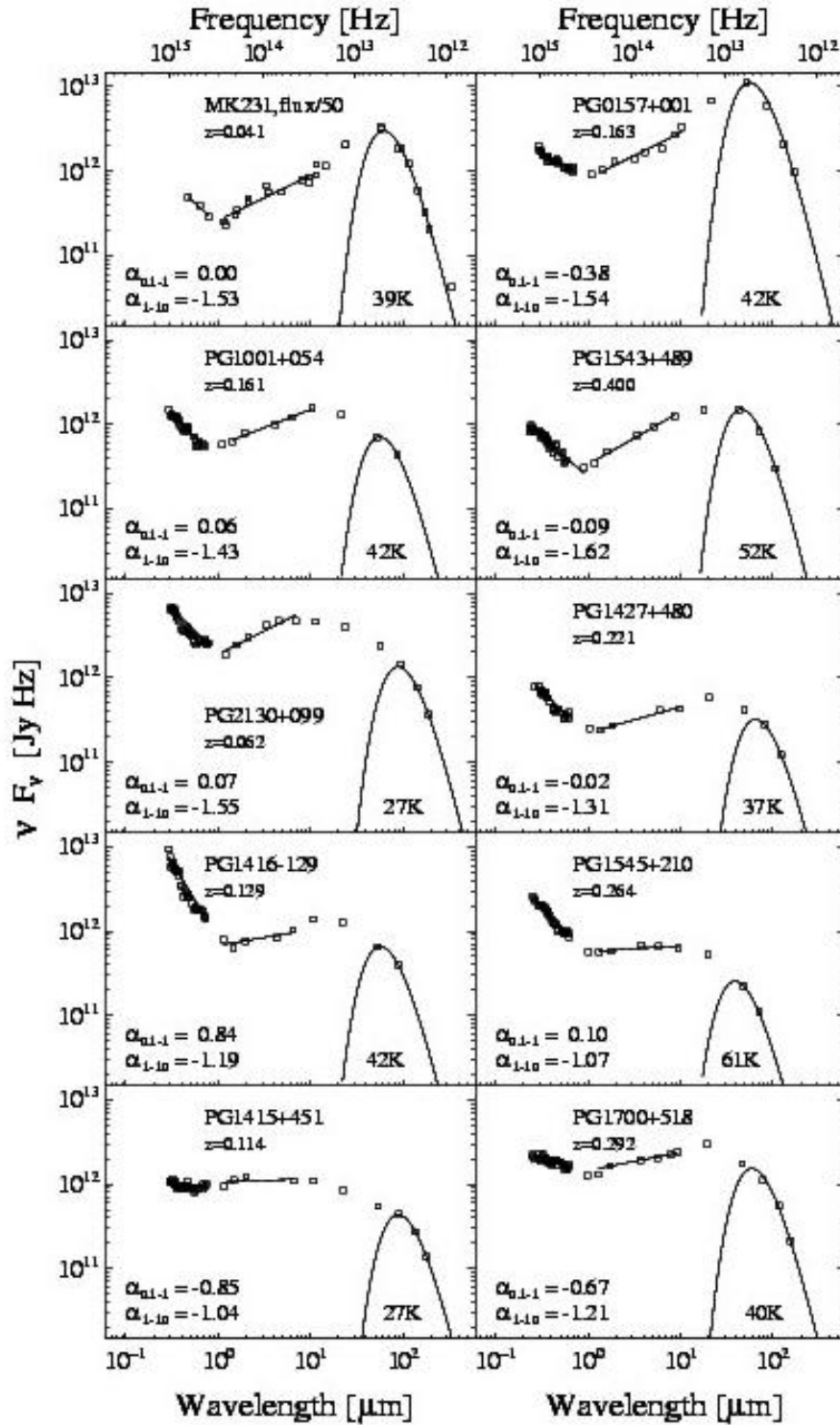


Figure 14: A fraction of the observed SED for low-redshift PG quasars (Haas et al. 2002).

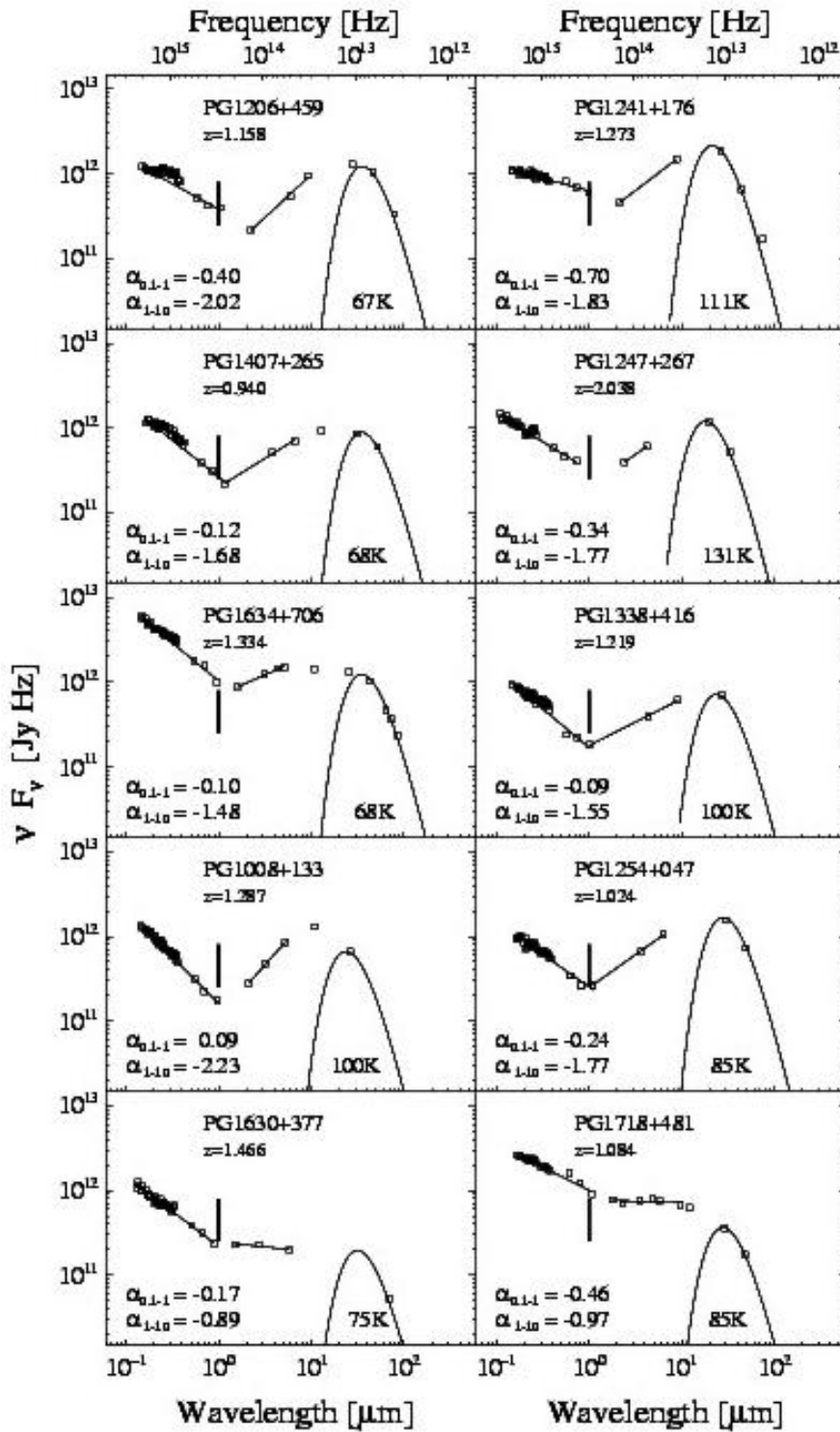


Figure 15: A fraction of the observed SED for medium-redshift PG quasars (Haas et al. 2002).

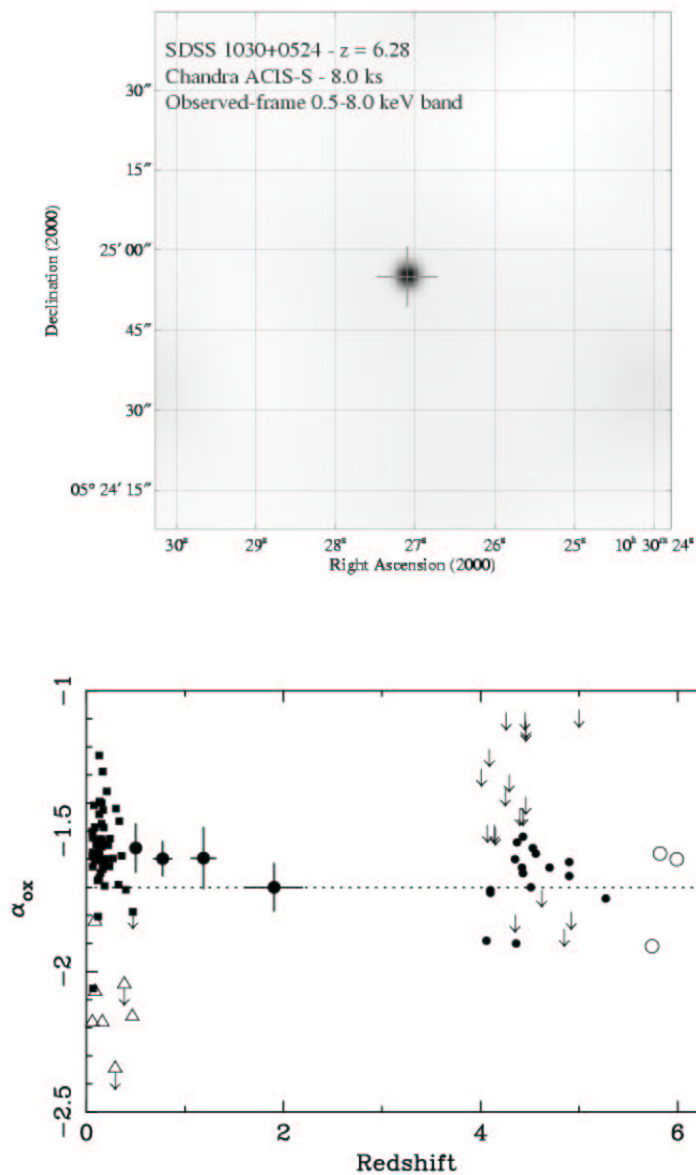


Figure 16: Low and high redshift Quasars in X-rays, plotted is the slope between the optical and X-ray spectrum. The upper panel shows the detection of the high-redshift Quasar with Chandra.

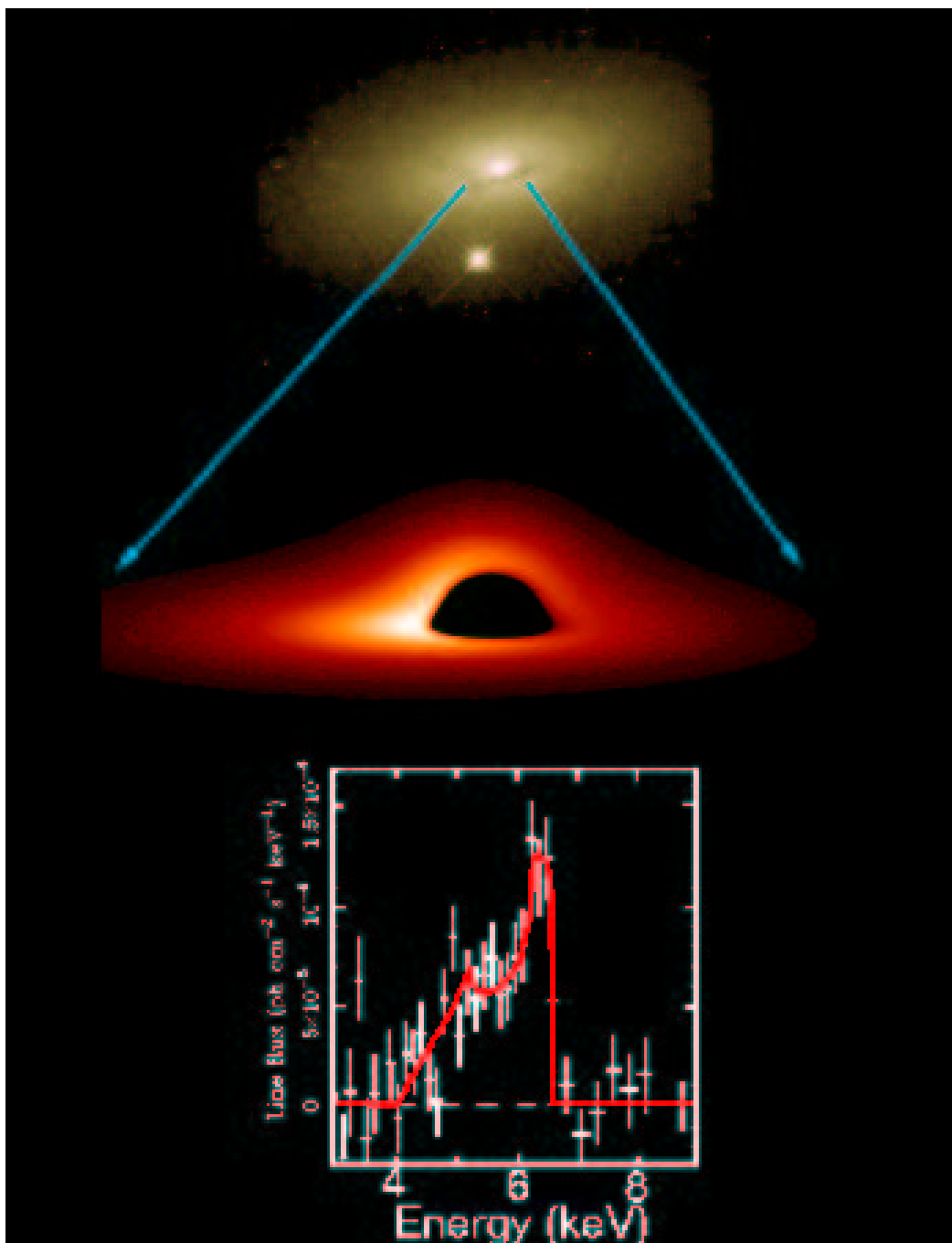


Figure 17: Line emission from a cool disk near a rotating black hole. If the disk were spatially resolved, we would detect the distortion in the imaging due to gravitational effects (middle panel). In fact, we can only observe the total emission from the disk surface, e.g. in the line of the 6.4 keV Fe emission (lower panel).

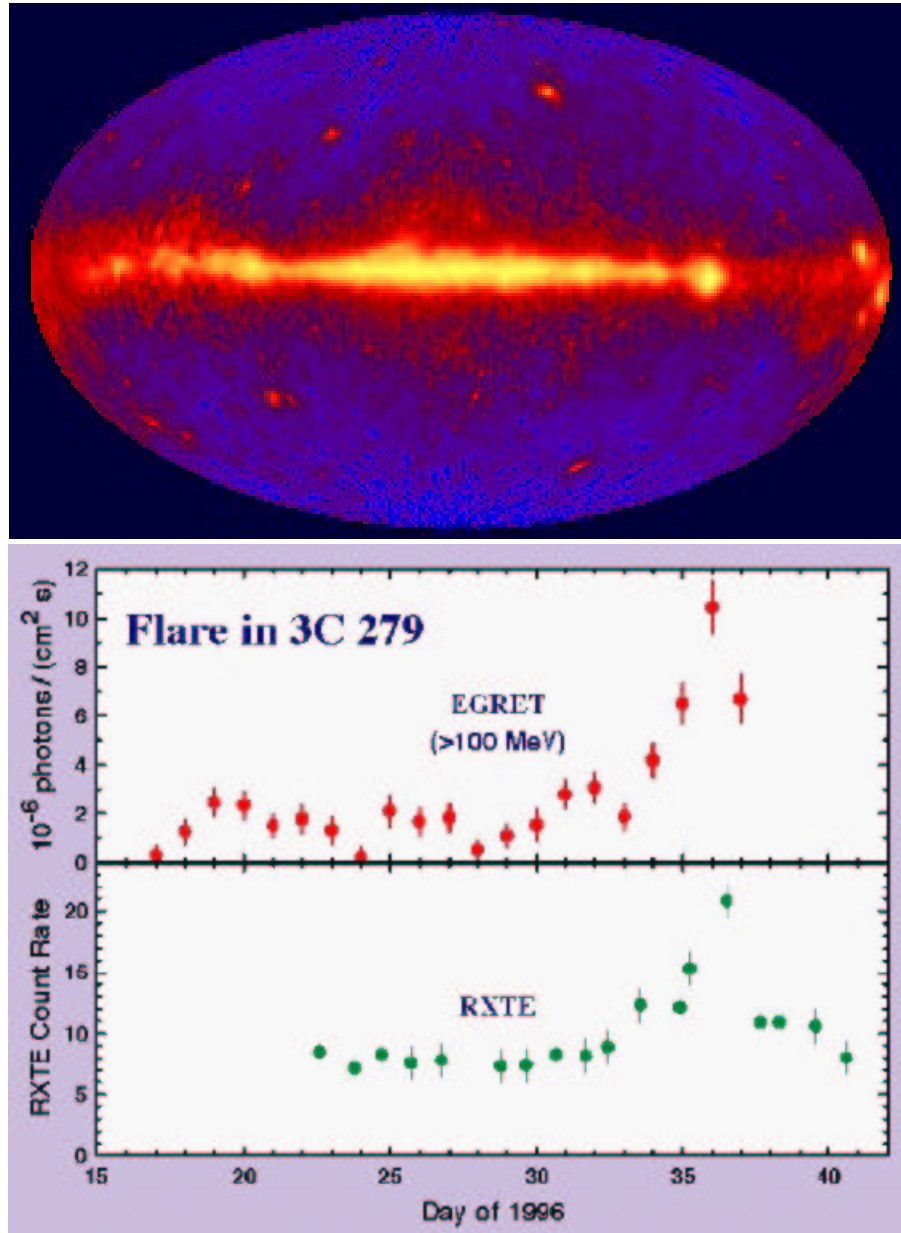


Figure 18: Gamma Ray Sky measured with EGRET (upper panel) and a flare in the emission of 3C 279 (lower panel). Most of the point sources detected by EGRET in the northern and southern galactic hemispheres are Quasars and BL Lac objects. 3C 279 shows pronounced flares in all wavebands, from radio to gamma-rays.

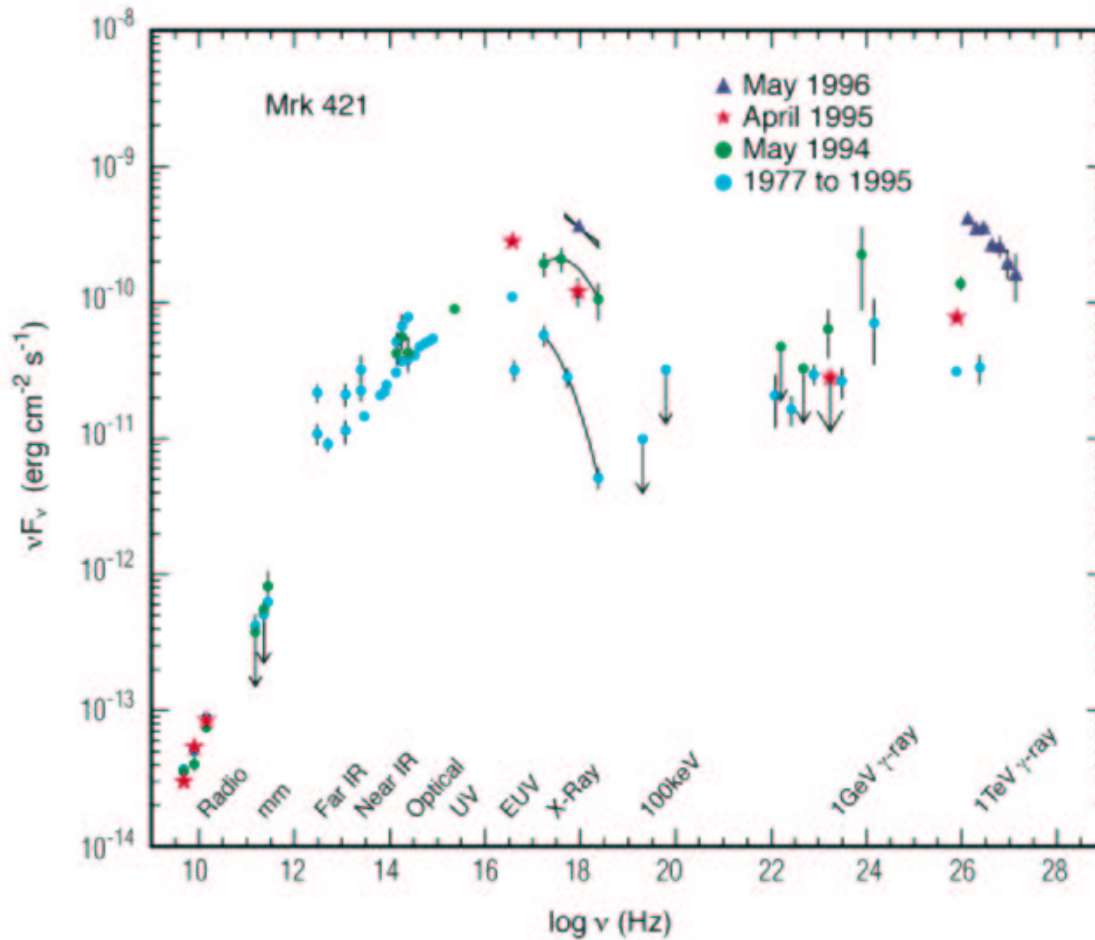


Figure 19: Global energy spectrum of the BL Lac object Mrk 421, which has a redshift of 0.033. Its host galaxy is a typical giant elliptical. In contrast to thermal Quasars, the spectra of BL lac objects are dominated by synchrotron emission from the radio regime into the optical region and by inverse Compton emission in the X-rays and Gamma-rays. In addition, the spectra are highly variable. These spectra are emitted by the relativistic plasma in the jets on the parsec-scale (so-called micro-jets).

1.4 Quasar Models

The actual standard model for Quasars and other types of active galactic nuclei is based on the existence of a supermassive Black Hole in the center of the host galaxy with masses $M_H \simeq (10^6 - 10^{10}) M_\odot$. The activity is driven by accretion of gas located on the parsec-scale in the core of the galaxy. Since this gas disposes of angular momentum, it streams in a disk towards the center, and not spherically symmetric. The inner edge of this disk is given by the Schwarzschild radius of the putative Black Hole

$$R_S = \frac{2GM_H}{c^2} = 2 \text{ AU} \frac{M_H}{10^8 M_\odot}. \quad (5)$$

Such Black Holes build therefore true holes in space in the center of a galaxy with the dimension of the solar system, depending on the mass involved.

From this scale, we also can derive a typical minimal characteristic time-scale

$$t_{\min} = \frac{R_S}{c} = 1000 \text{ sec} \frac{M_H}{10^8 M_\odot}. \quad (6)$$

This is of the order of a fraction of hours for Seyfert galaxies, as observed e.g. in the variability of the X-ray emission. The X-rays of Seyfert galaxies must therefore be generated in the immediate vicinity of the horizon of the Black Hole.

These accretion disks exist at least up to a radius of a few thousand Schwarzschild radii (i.e. about 0.01 light years) and make then probably a transition to a very turbulent regime, where self-gravity of the disk becomes important. This is exactly the region, where the broad emission lines are generated. The very fuel for the accretion disks is located on the scale of a few parsecs up to a few hundred parsecs. This is the interstellar medium of the core of the galaxy, which has probably a very complicated structure. It is certainly a multi-phase medium, where cool clouds are embedded into a hot X-ray gas with a temperature of about 0.2 keV (Figs. 20, 21). Due to the high turbulent velocities of these molecular clouds, this gas does not form a geometrically thin disk (as e.g. in our Galactic disk, where the turbulent velocity is only 10 km/s), but a torus-like geometrically thick disk consisting of many, many turbulent clouds. This structure is called a **molecular torus**. Originally, one thought that this disk is geometrically thin, but warped in order to catch sufficient UV-flux from the central source (this model is often referred to as the Caltech-model [17]).

Cores of galaxies are then determined by the following parameters:

- Mass M_C and core-radius R_c of the nuclear region in a galaxy;
- Mass M_H of the Black Hole (BH);
- Angular momentum J_H of the BH;
- Accretion rate \dot{M} of the surrounding disk;

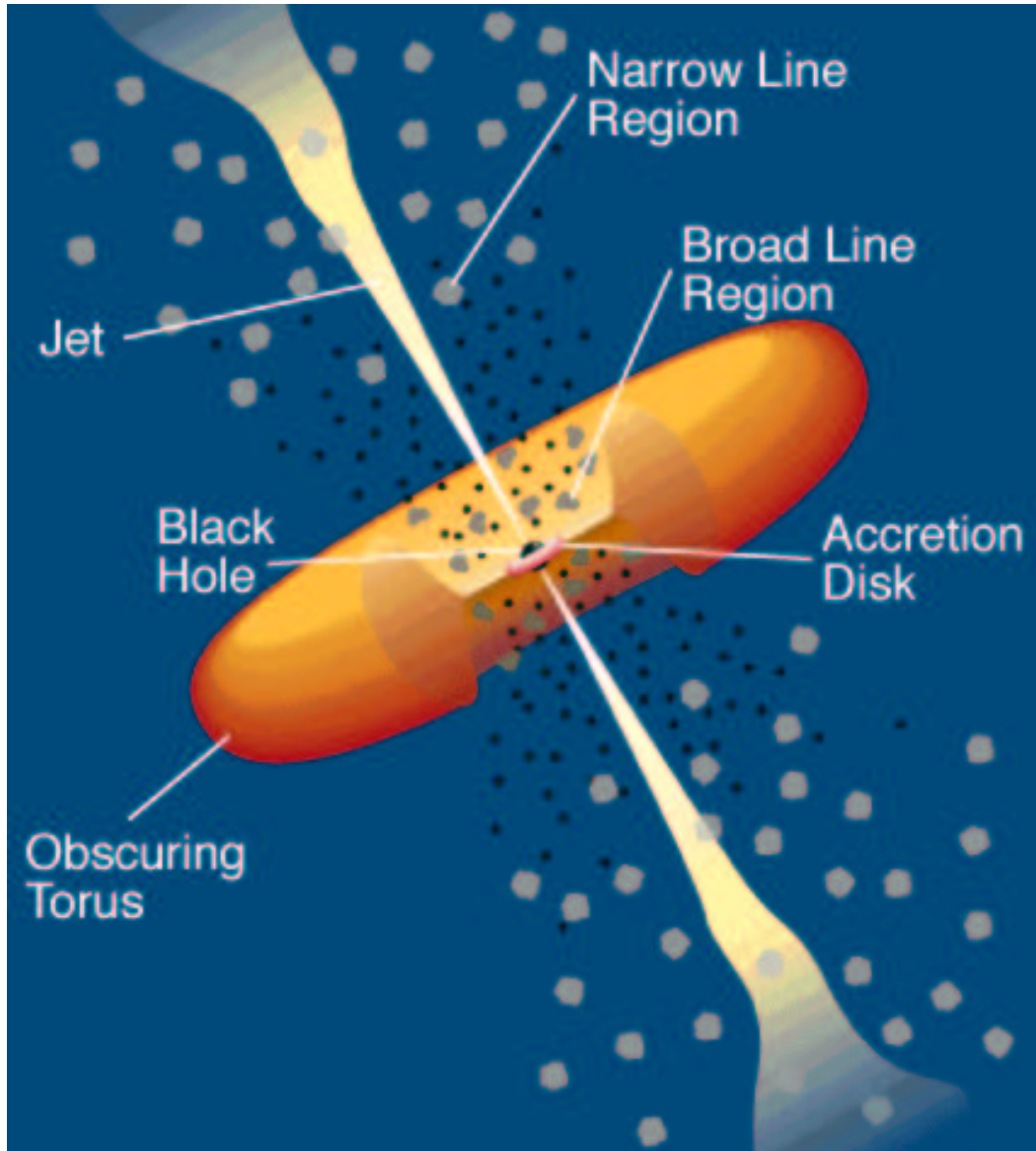


Figure 20: A very popular cartoon for modelling the structure of Quasars (Urry & Padovani 1995). Gas is assembled for some reasons in a torus-like structure on the parsec-scale. From here, accretion starts towards the central Black Hole. Some fraction of accreted gas is driven away to form jets. Broad emission lines (BLR) are located inside the torus so that they are hidden from direct view when seen edge-on. The narrow lines (NLR) are emitted by clouds moving on the scale of a few hundred parsecs.

- Inclination Θ of the line sight with the disk;
- Mass M_{Gas} of the molecular disk on the parsek-scale;
- Magnetic field B_D of the molecular torus (typically of the order of micro-Gauss).

Not all of these parameters are independent. So we expect that the mass in the molecular torus determines the accretion rate towards the center. And this accretion rate then determines the luminosity

$$L_N = \epsilon_H \dot{M} c^2 = 5 \times 10^{45} \text{ erg s}^{-1} \frac{\epsilon_H}{0.1} \frac{\dot{M}}{M_\odot \text{ yr}^{-1}} \simeq 1.2 \times 10^{12} L_\odot \frac{\dot{M}}{M_\odot \text{ yr}^{-1}}. \quad (7)$$

$\epsilon_H \simeq 0.1$ is the efficiency for transforming accretion into radiation. For optically thick disks, this efficiency is of the order of 10% for Black Holes. A bright Seyfert galaxy with $L_N \simeq 10^{12} L_\odot$ needs then about one M_\odot per year as fuel. Quasars need much more fuel, since their luminosities are upto a factor 100 higher than in Seyfert galaxies. There is a maximal luminosity for accretion following from the Eddington argument, which requires gravitational forces to be equilibrated by radiation pressure in a completely ionised gas

$$L_{ED} = \frac{4\pi G M_H m_p c}{\sigma_T} \simeq 1.3 \times 10^{46} \text{ erg s}^{-1} \frac{M_H}{10^8 M_\odot}. \quad (8)$$

Quasars contain therefore at least $(10^8 - 10^9) M_\odot$ in the central component, Seyfert galaxies need not have such high masses. Together with the accretion rate, we also can estimate a typical age for these sources

$$t_{\text{QSO}} \simeq \frac{M_H}{\dot{M}} \simeq 10^8 \text{ yr} \frac{M_H}{10^8 M_\odot} \left(\frac{\dot{M}}{M_\odot \text{ yr}^{-1}} \right)^{-1}. \quad (9)$$

Type I and Type II Quasars: The central region of galaxies cannot be completely spherically symmetric. The axisymmetric distribution of dust leads then to an inclination dependent optical depth towards the Quasar core. A torus is the simplest solution for this topological problem. At low inclination, the UV-hump of the inner accretion disk is not absorbed, while at higher inclination the whole UV will be absorbed by the dust in the torus. This was originally the idea to explain Seyfert type 1 and Seyfert type 2 galaxies by means of a simple **geometrical unification**. In Seyfert 2 galaxies, the broad emission lines are hidden behind the dusty torus. They can only be detected in polarised emission. A similar model should hold for Quasars. A typical Quasar is then only the type I object, where broad lines can be observed directly along the line of sight. In type II Quasars, broad lines should also be hidden behind the dusty torus, which has now been detected by means of its emission in the infrared. There should be at least as many type II

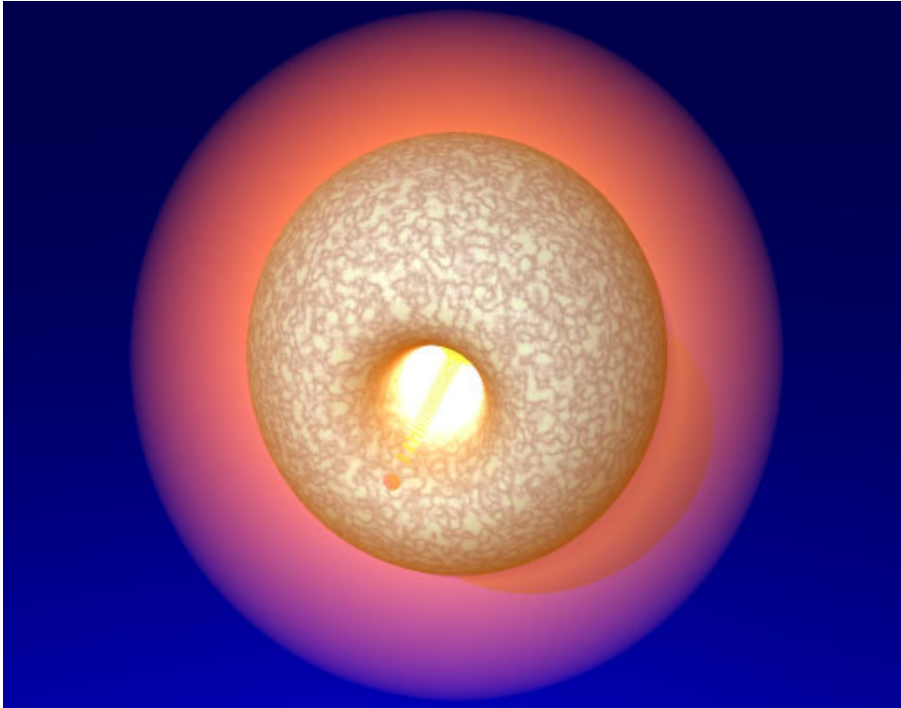


Figure 21: The structure of the core of elliptical galaxies (Camenzind 2001). The stellar distribution is roughly constant inside the core radius (red color), which is typically one kiloparsec in giant ellipticals. Gas and dust forms a toroidal structure (cloudy) due to the presence of some angular momentum in the gas. Since the total mass in the gas is much less than the total mass in stars, the gas distribution is a consequence of a mere mechanical equilibrium between pressure forces (turbulence), gravitational forces from the stars and the Black Hole and centrifugal forces.

Quasars as there are type I objects. The exact number depends on the structure of the molecular torus. The best way to find type II Quasars is over the search of hard X-rays, since they are not absorbed by the dust. In deep X-ray surveys, many of these objects have been found. The total number of Quasars is therefore much higher than estimated simply on grounds of optical surveys.

According to unified models of AGN, orientation and intrinsic luminosity (accretion rate) are the two primary physical parameters governing the optical characteristics of an active galaxy (Antonucci 1993; Urry & Padovani 1995). When the obscuring torus is oriented perpendicular to the observers line of sight, one sees spatially unresolved, Doppler boosted emission from hot gas near the central Black Hole in the form of broad (FWHM = 5000 – 20000 km/s) high-ionisation emission lines. Independent of the orientation, one sees narrow emission lines (FWHM = 500 – 1500 km/s) fromw spatially extended narrow line regions. When the line of sight is blocked by the torus, only the extended narrow line region is seen. Active galaxies without observed broad emission lines, but with high-ionisation species are classified

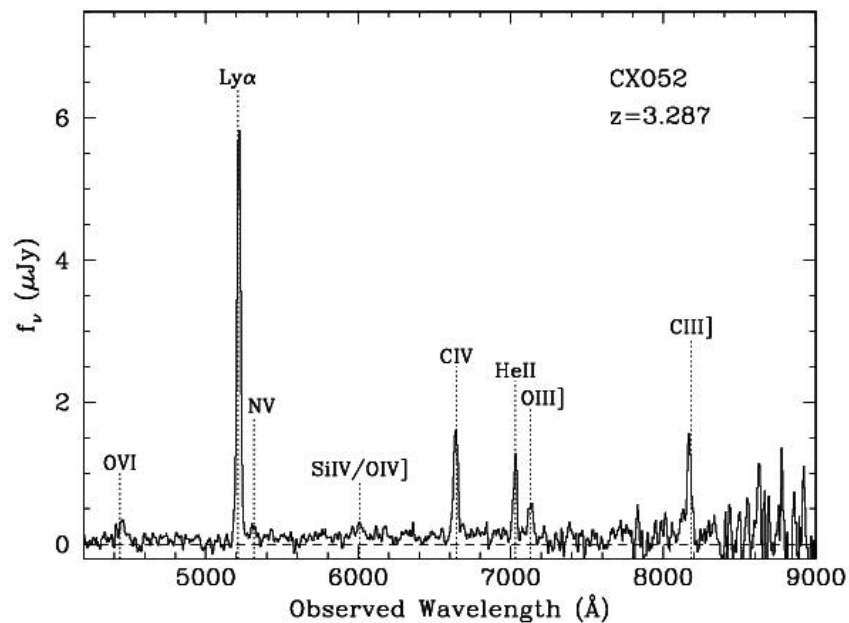
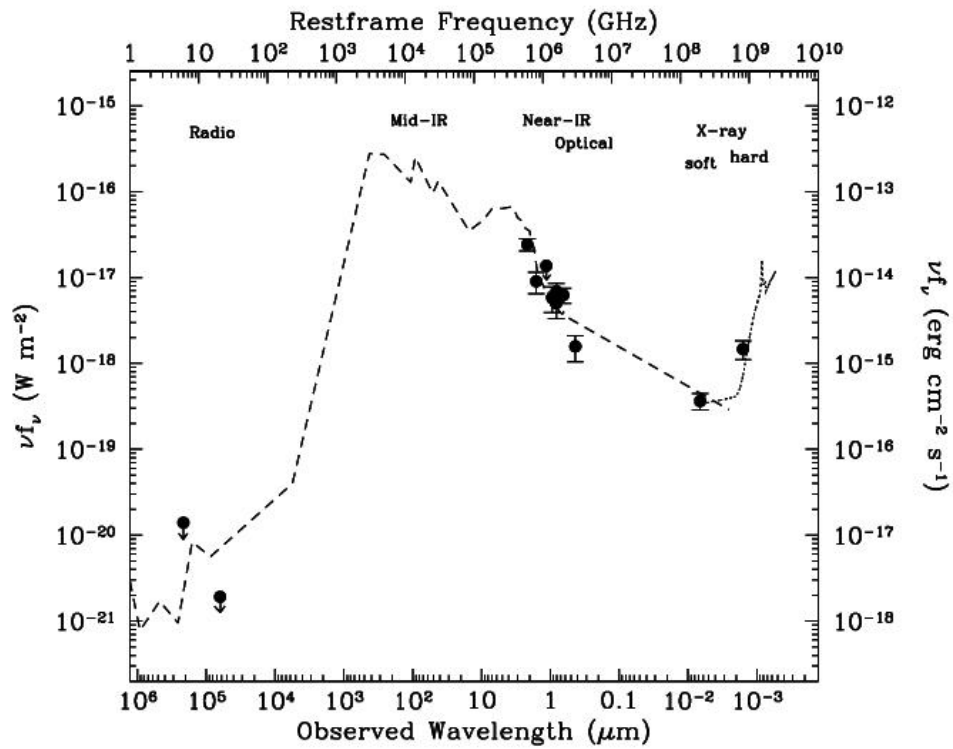


Figure 22: A Type II Quasar CX052 at redshift 3.287 detected in a Chandra deep field (Stern et al. 2002). Top panel: Photometry of CX052 plotted with the scaled average energy distribution (SED) of Seyfert II galaxies. Lower panel: Optical spectrum obtained with the Keck I telescope. The aperture used was $1.''5 \times 1.''5$.

as Type II systems, while those with broad lines as Type I systems. Hard X-rays, infrared and radio emission are also largely immune to obscuration and orientation effects. For spiral galaxies, the local ratio of obscured (Type II) to unobscured (Type I) Seyferts is roughly 4 : 1. In the case of Type II Quasars, our knowledge is still sparse. One way to find Type II objects at higher redshifts is by means of deep X-ray surveys.

Global Continua: The emission from the central accretion disk is responsible for the continuum observed in the optical, UV and soft X-ray regime of the spectrum (less than 0.5 keV). Dust in the torus on the parsec-scale will absorb some fraction of this emission and reprocess it to the infrared domain. This is the modern interpretation of the infrared hump observed from 100 to 1 μm in the energy distribution of Seyfert galaxies (first detected by IRAS) and PG Quasars (now detected with

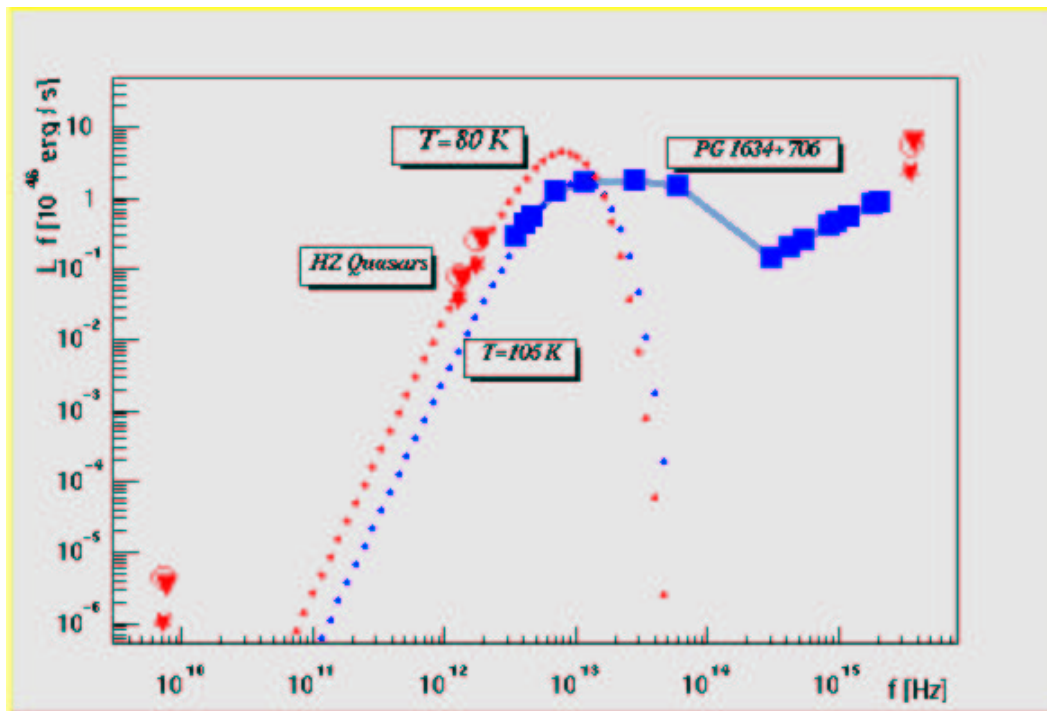


Figure 23: Energy distribution of the bright PG Quasar PG 1634+706 at redshift 1.2 and of 3 high redshift Quasars (Camenzind & Thiele 2002). The lowest temperature in the dust emission of the PG Quasar is about 100 K, quite similar to what is measured for higher redshift Quasars in the Rayleigh–Jeans regime. Since PG 1634+706 is a bright Quasar, we expect a similar dust spectrum for bright high-redshift Quasars. The optical emission of both types of Quasars is quite similar, apart from a factor 2 more luminous at high redshifts. The radio emission is down by six orders of magnitude and is completely irrelevant for the total energy budget.

ISOPHOT, Fig. 23). ISO was not sufficiently sensitive to detect this dust emis-

sion at redshifts beyond one. SIRTf will help to achieve this in the near future. Dust could however be detected in the low-frequency Rayleigh–Jeans regime with SCUBA at 450 and 800 μm for a few Quasars at redshift 4, corresponding to dust emitting at a temperature of about 100 K, quite similar to the lowest temperatures detected for PG Quasars [10].

Radio–Loud Quasars: All Quasars and Seyfert galaxies dispose of jets, i.e. of highly collimated bipolar plasma outflows. The existence of these jets is a generic phenomenon of active galactic nuclei, though the power involved in this phenomenon is different from source to source. High-power jets are known as radio–loud quasars (3C 273 e.g.) and bright radio galaxies (such as Cygnus A). The jets in radio–quiet Quasars and Seyfert galaxies are of low power compared to the bolometric luminosities of these sources. There seems to be a dichotomy in jet power, though in recent years sources have been found with intervening radio power. But anyway, no Seyfert galaxy has been found so far to show superluminal motion.

Red Quasars: Elusive red quasars may be more common than previously expected. Every massive galaxy is thought to have contained a quasar at some point in its lifetime. The gas near the horizon is so hot that quasars appear blue in colour. Red quasars have however smoke–like dust in front of them. This dust absorbs the blue light from the quasar, making it appear redder and fainter.

Red quasars are difficult to detect because their color make them hard to distinguish from stars. Lacy [13] used two surveys for this purpose, the Two Micron All–Sky survey (2mass) and the Faint Images of the Radio Sky at 20 cm (FIRST) conducted with the VLA. By comparing with the digitized Palomar Sky survey, they were able to catch up the optically faint quasars.

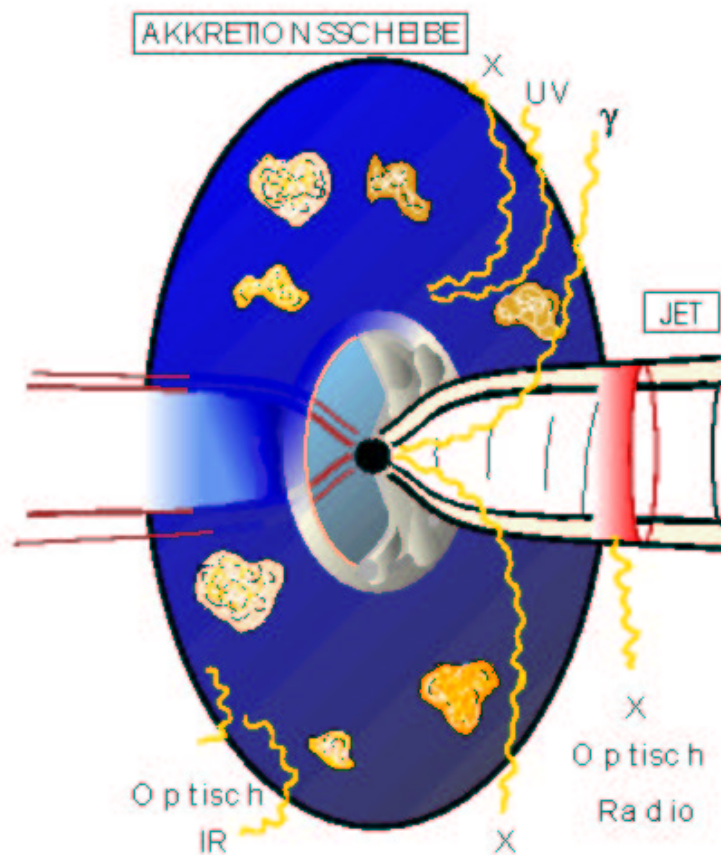


Figure 24: Falcke model for jet sources. Jets are driven by an inner hot accretion disk around a Black Hole. The hot plasma is collimated by magnetic fields on the sub-parsec-scale into cylindrical beams. Relativistic electrons in the beam emit synchrotron radiation, and low energy photons are scattered on these electrons to X-ray and gamma-ray regime.

References

- [1] Antonucci, R. 1993, AAR&A 31, 473
- [2] Bennett, A.S. 1961, MemRAS 68, 163
- [3] Brandt, et al. 2001, ApJ
- [4] Camenzind, M., Thiele, M. 2002, A&A, submitted
- [5] Curtis, H.D. 1913, Lick Obs. Publ. 13, 11
- [6] Edge, D.O. et al. 1959, MemRAS 68, 37
- [7] Ekers, J.A. 1969, Austr. J. Phys. Astroph. Suppl. No. 7, 1

- [8] Elvis, M. et al. 1994, ApJ Supp 95, 1
- [9] Haas, M., et al. 2000, A&A
- [10] Haas, M., et al. 2002, A&A, in press
- [11] Hazard, C., Mackey, M.B., Shimmins, A.J. 1963, Nature 197, 1073
- [12] Hewitt, A., Burbidge, G. 1997, ApJ Supp 87, 451
- [13] Lacy, M. et al. 2002, astro-ph/0203065
- [14] Meisenheimer, K. et al. 2001, A&A 372, 719
- [15] Pounds, K., Reeves, J. 2002, astro-ph/0201436
- [16] Salpeter, E.E. 1964, ApJ 140, 796
- [17] Sanders, Phinney, Neugebauer, Soifer, Matthews, 1989, ApJ 347, 29
- [18] Schmidt, M. 1963, Nature 197, 1040
- [19] Schmidt, M., Green, R.F. 1983, ApJ 269, 352
- [20] Seyfert, C., 1943, ApJ 97, 28
- [21] Stern, D. et al. 2002, astro-ph/0111513
- [22] Urry, C.M., Padovani, P. 1995, "Unified Schemes for Radio-Loud Active Galactic Nuclei", PASP, 107, 803
- [23] Vanden Berk, D.E. et al. 2001, astro-ph 0105231
- [24] Woltjer, L. 1959, ApJ 130, 38
- [25] Zel'dovich, Ya.B., Novikov, I.D. 1964, Sov. Phys.Dokl. 158, 811
- [26] Zheng, W. et al. 1997, ApJ,